Endothelial Sirt1 Is Required for PGC1α-Induced Angiogenesis in Skeletal Muscle Tissue

Citation
Huang, George. 2017. Endothelial Sirt1 Is Required for PGC1α-Induced Angiogenesis in Skeletal Muscle Tissue. Doctoral dissertation, Harvard Medical School.

Permanent link
http://nrs.harvard.edu/urn-3:HUL.InstRepos:32676114

Terms of Use

Share Your Story

Accessibility

ACKNOWLEDGMENTS

With gratitude,

George X. Huang
M.D. Candidate
Harvard Medical School, Class of 2017

CONTENTS

ABSTRACT

It is believed that the health benefits of exercise are mediated in part by exercise-induced adaptations of skeletal muscle tissue. The mechanisms whereby alterations in cellular energy state are sensed and how these signals are then transduced into physiologic adaptations of skeletal muscle are subjects of intense investigation. Sirtuin 1 (Sirt1) is an NAD^+-dependent deacetylase that regulates cellular energy output. Based on *in vitro* studies performed using C2C12 myoblasts, it is widely assumed that Sirt1 in skeletal myofibers is required for activating PGC1α, a transcriptional coactivator that potently stimulates mitochondrial biogenesis and the release of angiogenic factors in response to exercise. We propose that Sirt1 within skeletal myofibers is not required for the activity of PGC1α *in vivo*, and we hypothesize instead that Sirt1 within endothelial cells is required for PGC1α-induced angiogenesis in skeletal muscle tissue.

To investigate this hypothesis, overexpression of PGC1α in skeletal myofibers (MCK-PGC1α) was used to simulate exercise training in mice lacking Sirt1 activity in skeletal myofibers (Sirt1flox Myog-Cre) or endothelial cells (Sirt1flox Tie2-Cre). The activity of PGC1α was not suppressed by knockout of Sirt1 in skeletal myofibers, as evaluated by qPCR analysis of oxidative metabolism genes, Western blotting of proteins of oxidative phosphorylation, quantification of cross-sectional vascular density in skeletal muscle tissue, and treadmill endurance testing. In contrast, knockout of Sirt1 in endothelial cells resulted in impaired angiogenesis in response to PGC1α overexpression, as evaluated by quantification of vascular density within the quadriceps muscle group. Thus, we conclude that Sirt1 within skeletal myofibers is not required for PGC1α activity when PGC1α is overexpressed *in vivo*; however, endothelial Sirt1 is required for angiogenesis within skeletal muscle tissue in response to PGC1α, an essential mediator of exercise-induced angiogenesis. Furthermore, we demonstrate that, in MS1 endothelial cells, Sirt1 appears to regulate chemotaxis through Notch-independent pathways.

Ultimately, these findings identify endothelial Sirt1 as a key regulator of angiogenesis in skeletal muscle tissue and as a new therapeutic target for diseases of vascular insufficiency. In addition to further characterizing the mechanism by which endothelial Sirt1 modulates angiogenic behavior, our current studies now seek to characterize the effects of administering nicotinamide mononucleotide (NMN), a pharmacologic activator of Sirt1, in mice with age-

associated endothelial dysfunction and in mouse models of hindlimb ischemia. This has therapeutic potential for peripheral artery disease, myocardial ischemia, and vascular diseases of the central nervous system.

INTRODUCTION

Background

Systemic health benefits of endurance exercise include decreased risk of cardiovascular disease, improved insulin sensitivity, prevention of age-associated sarcopenia and lipodystrophy, decreased low-grade chronic inflammation, and even prevention of neurological symptoms in patients with mitochondrial myopathies.(1-3) It is believed that these health benefits are mediated in part by exercise-induced adaptations of skeletal muscle tissue. The mechanisms whereby alterations in cellular energy state are sensed and how these signals are then transduced into coordinated physiological adaptations in skeletal muscle tissue are the subjects of the intense of investigation.

The mammalian Sirtuin family consists of seven evolutionarily conserved proteins (Sirt1-Sirt7) which regulate whole-body metabolic homeostasis and stress resistance.(4) Of these, Sirt1 is the mammalian ortholog of Sir2, a protein that has been found to regulate longevity in response to caloric restriction in *S. cerevisiae*, *C. elegans*, and *D. melanogaster*.(5, 6) Specifically, Sirt1 is an NAD^+-dependent deacetylase that regulates cellular energy output and metabolic homeostasis. Known target proteins of deacetylation by Sirt1 include the tumor suppressor p53, the Notch intracellular domain (NICD), as well as transcription factors of the FOXO and LXR families.(4)

Recently, it has also been discovered that Sirt1 can deacetylate and thereby activate peroxisome proliferator-activated receptor-γ coactivator-1α (PGC1α), a transcriptional coactivator that upregulates oxidative metabolism in a wide variety of tissues. In particular, in extracts from mouse liver tissue, Sirt1 has been demonstrated to regulate expression of gluconeogenic genes through directly deacetylating PGC1α at several lysine residues.(7) Similarly, in HeLa cells, Sirt1 regulates oxygen consumption by directly deacetylating PGC1α.(8) In these contexts, deacetylation by Sirt1 is thought to activate PGC1α by enabling translocation into the nucleus, where PGC1α acts to regulate gene expression.(9)

In skeletal myofibers, PGC1α is strongly induced by exercise and β-adrenergic signaling,(10, 11) and it functions to enhance exercise performance through potently stimulating mitochondrial biogenesis and the release of angiogenic factors.(12, 13) Given the important roles of PGC1α in skeletal muscle, it is thought that Sirt1 may coordinate the physiological

adaptations of skeletal muscle tissue to exercise through deacetylating and thereby activating PGC1α in skeletal myofibers.

State of the Field

Several *in vitro* studies support such a role for Sirt1. In C2C12 myotubes, upregulation of oxidative metabolism genes in response to treatment with resveratrol (an allosteric activator of Sirt1) requires the presence of PGC1α, suggesting that PGC1α lies downstream of Sirt1 activity in these cells.(14) Furthermore, multiple groups have reported that upregulation of mitochondrial genes by adenoviral-mediated overexpression of PGC1α in C2C12 myotubes is blocked when Sirt1 expression is knocked down by shRNA,(14, 15) suggesting that Sirt1 is required for activity of PGC1α in these cells. Finally, deacetylation of PGC1α by Sirt1 is required for activation of PGC1α by AMP-activated protein kinase (AMPK) in C2C12 myotubes.(16) These *in vitro* results, obtained using immortalized cell lines, have led to the prevailing model that Sirt1 in skeletal myofibers is required for the activation of PGC1α.

However, this role for Sirt1 in skeletal myofibers has yet to be convincingly validated *in vivo*, and remains a source of great controversy.(17-19) A mouse knockout model of Sirt1 activity (Sirt1flox), in which exon 4 (which encodes the catalytic domain of the protein) of the Sirt1 gene is flanked by LoxP sequences, was created in 2003,(20) allowing groups to investigate the functions of Sirt1 in skeletal muscle *in vivo* by using Cre recombinases driven by inducible and/or muscle-specific promoters (see **Figure 1**). Gomes et al. examined skeletal muscle from mice with inducible whole body knockout of Sirt1 exon 4 (Sirt1flox ERT2-Cre) and found decreased levels of mitochondrial-encoded but not nuclear-encoded genes of oxidative metabolism.(21) However, this regulation of mitochondrial-encoded genes by Sirt1 still occurs in primary myotubes isolated from mice lacking PGC1α, and instead operates through the ability of Sirt1 to stabilize HIF-1α rather than through interaction of Sirt1 with PGC1α.(21) Menzies et al. reported that exercise-induced mitochondrial biogenesis in skeletal muscle is preserved in mice with type II myofiber-specific deletion of Sirt1 exon 4 (Sirt1flox MLCf1-Cre),(22) but this finding is difficult to interpret because it has since been revealed that PGC1α is not actually required for exercise-induced mitochondrial biogenesis *in vivo*.(23) Philp et al. reported no impairments in deacetylation of PGC1α in response to exercise training in mice with skeletal myofiber-specific deletion of Sirt1 exon 4 (Sirt1flox MCK-Cre), but their findings are not widely recognized because they failed to demonstrate deletion of Sirt1 exon 4 at the protein level.(24) Finally, Chalkiadaki et al. found that mice with skeletal myofiber-specific deletion of Sirt1 exon

4 (Sirt1flox MCK-Cre) exhibit decreased endurance capacity in treadmill tests,(25) but they did not evaluate whether this effect was mediated by regulation of PGC1α.

Thus, the prevailing model that Sirt1 deacetylates PGC1α in skeletal myofibers is based entirely upon *in vitro* studies using immortalized cell lines, and it currently remains unknown whether Sirt1 is required for activating PGC1α in skeletal myofibers *in vivo*. Here, given that Sirt1 in skeletal myofibers possesses the ability to regulate oxidative metabolism independently of PGC1α and that PGC1α is not required for mitochondrial biogenesis in response to voluntary wheel running,(21, 23) further studies using transgenic animal models in which Sirt1 exon 4 is deleted and PGC1α is simultaneously overexpressed within skeletal myofibers are required to clarify this physiologic role of Sirt1 *in vivo*.
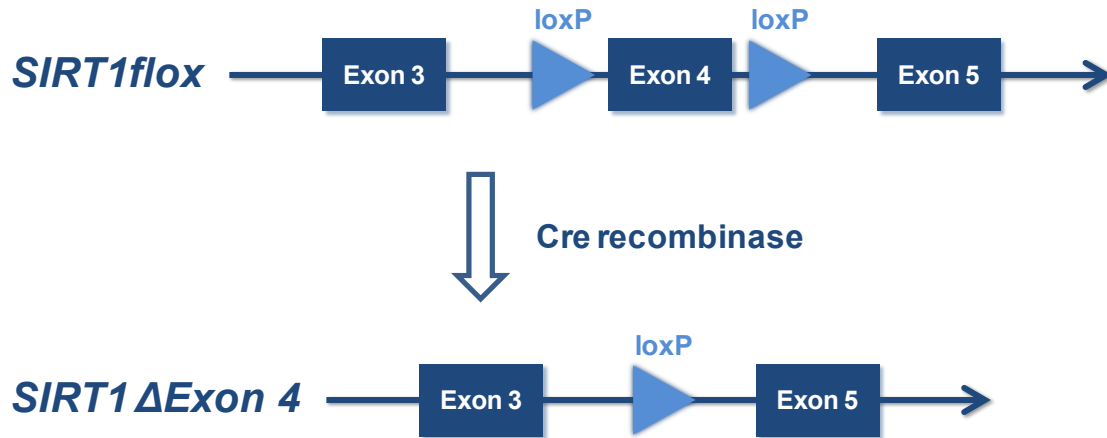
Figure 1: Cre-Lox Recombination System for Sirt1 Exon 4

Exon 4 (which encodes the catalytic domain) of the SIRT1 gene is flanked with LoxP sequences for site-specific recombination. In the presence of Cre recombinase, which can be expressed in an inducible or tissue-specific manner, exon 4 is excised from the SIRT1 gene locus.

Alternatively, Sirt1 may facilitate adaptations of skeletal muscle tissue to exercise through its activity in endothelial cells rather than in skeletal myofibers. Sirt1 is highly expressed in the endothelium (26, 27) and although most studies have examined endothelial Sirt1 in the context of promoting vasodilation via activating endothelial nitric oxide synthase (eNOS),(28) some recent work has begun to elucidate an emerging role for endothelial Sirt1 in regulating vascular density and angiogenic behavior. Specifically, *in vitro* siRNA knockdown of Sirt1 blocks sprouting angiogenesis in human umbilical vein endothelial cells (HUVECs) and in mouse lung cancer endothelial cells.(26, 29) Additional studies have demonstrated that endothelial Sirt1 promotes angiogenic behavior through deacetylating the Notch intracellular domain (NICD), thereby enhancing proteolytic degradation of NICD and ultimately inhibiting downstream Notch signaling.(27)

Recent studies also hint that endothelial Sirt1 is required for proper angiogenesis *in vivo*. Specifically, mice with endothelium-specific deletion of Sirt1 exon 4 (Sirt1flox Tie2-Cre) exhibit impairments in postnatal angiogenesis within the retina and defective neovascularization in response to hindlimb ischemia.(26, 27) However, the extent to which endothelial Sirt1 regulates microvascular remodeling in skeletal muscle tissue in response to factors such as exercise and PGC1α remains to be explored. Here, given that PGC1α mediates and is required for exercise-induced angiogenesis in skeletal muscle tissue,(13) transgenic animal models in which

overexpression of PGC1α in skeletal myofibers is used to stimulate angiogenesis and Sirt1 exon 4 is simultaneously deleted within endothelial cells offer an invaluable tool for investigating this role of Sirt1.

Hypothesis

We propose that Sirt1 within skeletal myofibers is not required for the activity of PGC1α *in vivo*. Alternatively, we hypothesize that Sirt1 within endothelial cells is required for angiogenesis in skeletal muscle tissue in response to PGC1α *in vivo*.

Diagrams of the prevailing model and our alternative hypothesis for the roles of Sirt1 in skeletal muscle tissue are shown in **Figure 2A** and **Figure 2B**, respectively. In this investigation, we use skeletal myofiber-specific and endothelium-specific animal knockout models of Sirt1 in order to clarify these physiologic roles of Sirt1 in mediating the PGC1α-induced adaptations of skeletal muscle tissue.
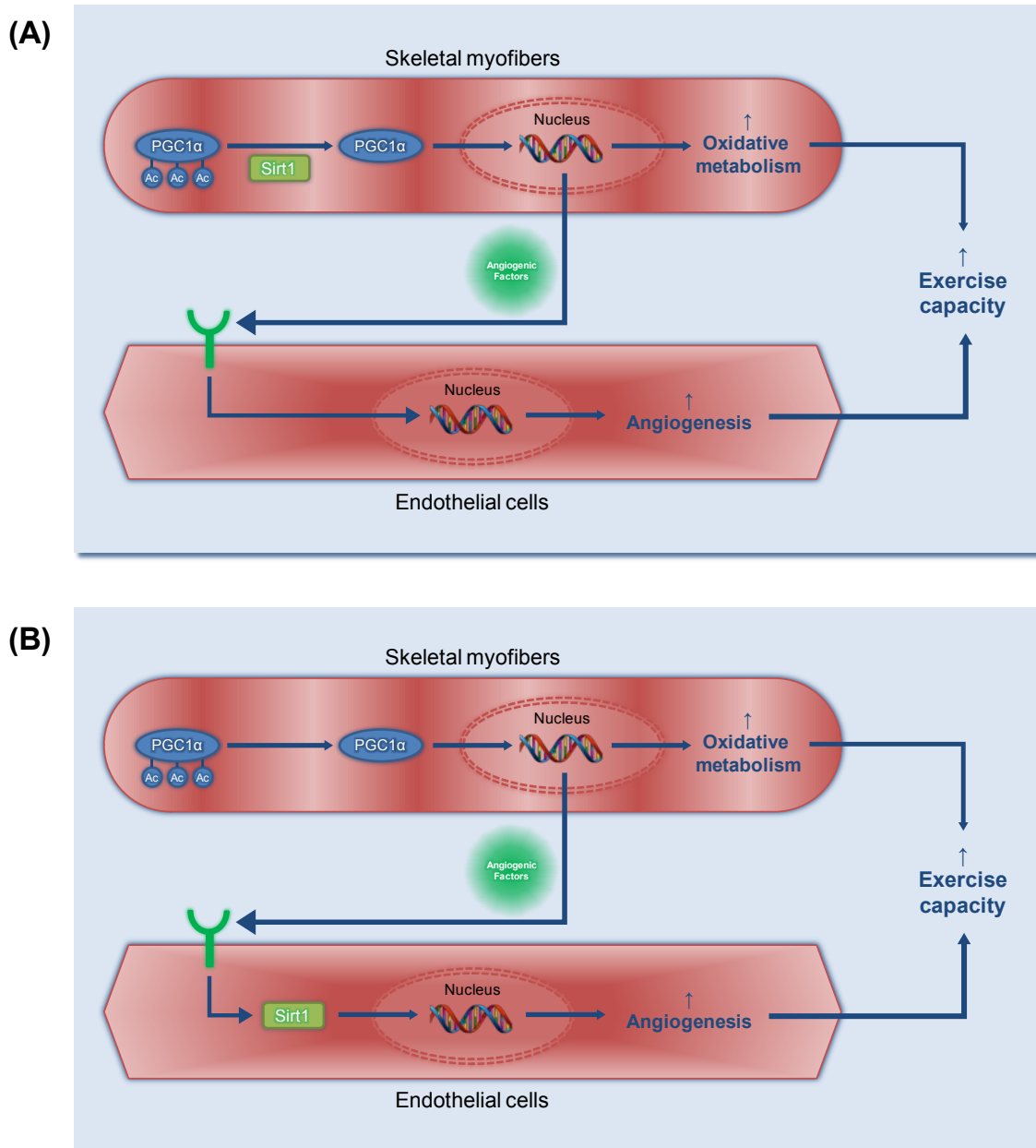
Figure 2: Possible roles of Sirt1 in regulating adaptations of skeletal muscle tissue in response to PGC1α.

(A) In the prevailing model of Sirt1 activity in skeletal muscle tissue, Sirt1 within skeletal myofibers is required for deacetylating and thereby activating PGC1α. Activated PGC1α then coordinates mitochondrial biogenesis and secretion of angiogenic factors (e.g. VEGF) in order to enhance exercise capacity. (B) In our hypothesized model of Sirt1 activity in skeletal muscle tissue, Sirt1 within skeletal myofibers is not required for PGC1α-induced upregulation of mitochondrial biogenesis and secretion of angiogenic factors. However, Sirt1 within endothelial cells is required for angiogenesis in response to angiogenic factors secreted in response to PGC1α.

Specific Aims

Aim 1: To evaluate the ability of PGC1α to upregulate oxidative metabolism in skeletal muscle tissue from mice that lack Sirt1 activity in skeletal myofibers.

As a preliminary study, primary myofibers with deletion of Sirt1 exon 4 were produced by isolating primary myoblasts from Sirt1flox mice, differentiating the myoblasts into myofibers, and then transducing the myofibers with adenoviral expression constructs for Cre recombinase. The ability of adenoviral-mediated overexpression of PGC1α to upregulate genes of oxidative metabolism in these myofibers was evaluated by quantitative reverse transcription polymerase chain reaction (RT-qPCR). Mice that simultaneously harbor deletion of Sirt1 exon 4 in skeletal myofibers and overexpress PGC1α in skeletal myofibers (Sirt1flox MCK-PGC1α Myog-Cre) were produced by several generations of breeding Sirt1flox mice (in which exon 4 of the SIRT1 gene, which encodes the catalytic domain of the Sirt1 protein, is flanked by LoxP recombination sequences), Myog-Cre mice (in which the expression of Cre recombinase is driven by the skeletal myofiber-specific myogenin promoter), and MCK-PGC1α mice (in which overexpression of PGC1α is driven by the skeletal myofiber-specific creatine kinase promoter). Deletion of Sirt1 exon 4 in skeletal myofibers of these mice was confirmed at the DNA, mRNA, protein, and enzymatic activity levels. The effects of PGC1α overexpression in these mice were evaluated in skeletal muscle tissue by RT-qPCR analysis for genes of oxidative metabolism, Western blotting for proteins of oxidative phosphorylation, immunofluorescence for cross-sectional vascular density, and treadmill endurance testing.

Aim 2: To evaluate PGC1α-induced angiogenesis in skeletal muscle tissue from mice that lack Sirt1 activity in endothelial cells.

Mice that simultaneously harbor deletion of Sirt1 exon 4 in endothelial cells and overexpress PGC1α in skeletal myofibers (Sirt1flox MCK-PGC1α Tie2-Cre) were produced by several generations of breeding Sirt1flox mice, Tie2-Cre mice (in which the expression of Cre recombinase is driven by the endothelial cell-specific angiopoietin receptor promoter), and MCK-PGC1α mice. Deletion of Sirt1 exon 4 in the endothelium of these mice was confirmed at the DNA, mRNA, and protein levels. The effects of PGC1α overexpression in these mice were evaluated in skeletal muscle tissue by RT-qPCR analysis for genes of oxidative metabolism,

Western blotting for proteins of oxidative phosphorylation, immunofluorescence for cross-sectional vascular density, and treadmill endurance testing.

Aim 3: To characterize whether Sirt1 regulates angiogenic behavior via modulating Notch signaling in MS1 murine endothelial cells.

Knockdown of Sirt1 expression in a mouse endothelial cell line (MS1) was performed via siRNA transfection. Knockdown of Sirt1 was verified by qRT-PCR, Western blotting, and immunofluorescence. An *in vitro* scratch or "wound healing" assay was used to assess how Sirt1 knockdown affected directional migration of MS1 cells into the scratch site, and a Transwell migration assay was used to quantify how Sirt1 knockdown affected chemotaxis toward a gradient of vascular endothelial growth factor (VEGF) or conditioned media produced by differentiated C2C12 myotubes. In addition, MS1 cells were treated with DAPT, a γ-secretase inhibitor that inhibits Notch signaling, and subjected to a Transwell migration assay in order to evaluate whether Notch signaling lies downstream of Sirt1 in MS1 endothelial cells.

MATERIALS AND METHODS

Reagents

Unless otherwise specified, all reagents were obtained from Sigma-Aldrich (St. Louis, MO).

Primary Myoblast Cell Culture and Transduction

Primary myoblasts were isolated from entire murine hindlimb muscle tissues. Briefly, hindlimb muscle was minced using scissors, enzymatically digested with type II collagenase (Roche Life Science, Indianapolis, IN) and dispase (Roche Life Science), and mechanically triturated. The resulting cell suspension was passed through a cell strainer with 70 μm pore size (Corning Life Sciences, Corning, NY). Cells in the filtrate were pelleted by centrifugation at 2000 RPM for 5 min, resuspended in Ham's F10 medium (Life Technologies, Carlsbad, CA), and cultured in Petri dishes (Corning Life Sciences). After 30 min, non-adherent cells were removed from the flask, pelleted by centrifugation at 2000 RPM for 5 min, resuspended in F10 medium, and cultured in collagen-coated dishes. The primary myoblasts were maintained in F10 medium (Life Technologies) supplemented with 20% fetal bovine serum (FBS), 100 IU/mL penicillin, and 100 mg/mL streptomycin at 37°C in a humidified incubator with 5% CO_2. Myoblasts were differentiated in Dulbecco's modified eagle medium (DMEM) (Life Technologies) supplemented with 5% heat-inactivated horse serum. The differentiated myotubes were then infected with adenoviruses expressing Cre recombinase, green fluorescent protein (GFP), and/or PGC1α at a multiplicity of infection (MOI) of 10-30. Adenoviruses expressing Cre recombinase and GFP were obtained from the Harvard Gene Therapy Initiative, while the adenovirus expressing PGC1α was a gift from Dr. Bruce Spiegelman (Dana Farber Cancer Center, Boston, MA).

Animal Experiments

All experiments were performed according to procedures approved the Institutional Animal Care and Use Committees (IACUCs) at the Beth Israel Deaconess Medical Center (Boston, MA) and the Harvard Center for Comparative Medicine (Boston, MA). Mice were housed in a standard animal maintenance facility under a 12 hour light-dark cycle, and fed a standard chow diet. All mice were maintained in the C57BL/6J genetic background. Mice

homozygous for the Sirt1 allele with LoxP sequences flanking exon 4 (Sirt1flox, 008041) and mice in which Cre recombinase was expressed under control of the endothelial cell-specific promoter for the angiopoietin receptor (Tie2-Cre, 008863) were purchased from the Jackson Laboratory (JAX Mice, Bar Harbor, ME). Mice in which Cre recombinase was expressed under control of the myofiber-specific myogenin promoter and MEF2C enhancer (Myog-Cre) were a gift from Dr. Eric N. Olson (UT Southwestern, Dallas, TX), and mice in which PGC1α was expressed under the skeletal myofiber-specific muscle creatine kinase promoter (MCK-PGC1α) were a gift from Dr. Bruce Spiegelman (Dana Farber Cancer Center, Boston, MA).

Sirt1flox MCK-PGC1α mice were generated by crossing Sirt1flox mice with the MCK-PGC1α mice for two generations to achieve homozygosity of the Sirt1flox allele. Sirt1flox Myog-Cre and Sirt1flox Tie-2Cre mice were generated by crossing female Sirt1flox mice with male Myog-Cre and Tie2-Cre mice, respectively, for two generations to achieve homozygosity of the Sirt1flox allele. Study groups were then produced by crossing female Sirt1flox MCK-PGC1α mice with male Sirt1flox Myog-Cre or male Sirt1flox Tie2-Cre mice (see **Figure 3**). All experiments were then performed on male mice at the age of 4 months.

Figure 3: Mouse Study Groups

Male Sirt1flox Myog-Cre or Sirt1flox Tie2-Cre mice were crossed with female Sirt1flox MCK-PGC1α mice in order to produce cohorts for study.

Quantitative Polymerase Chain Reaction (qPCR)

Total gDNA was isolated from samples using DNEasy (Qiagen, Valencia, CA), while total mRNA was isolated from tissues using TRIzol (Life Technologies) and from cultured cells using TurboCapture (Qiagen). Samples for RT-qPCR were then reverse transcribed using the High Capacity cDNA Reverse Transcription Kit (Life Technologies). qPCR was performed on the gDNA or cDNA with iQ SYBR Green Supermix (Bio-Rad, Hercules, CA) using the CFX384 Real-Time PCR Detection System (Bio-Rad) according to the manufacturer's instructions. Relative gDNA and mRNA expression levels were calculated using the $\Delta\Delta$Ct method. The forward and reverse primer sequences used in qPCR amplification reactions are displayed in **Table 1**.

Table 1: Primer sequences used in qPCR amplification reactions

Gene	Forward Primer (5' → 3')	Reverse Primer (5' → 3')
Hypoxanthine-guanine phosphoribosyltransferase (HPRT)	GTTAAGCAGTACAGCCCCAAA	AGGGCATATCCAACAACAAACTT
Ribosomal protein, large, P0 (36B4)	GGCTCCAAGCAGATGCAGCAG	CCTGATAGCCTTGCGCATCATGG
TATA-box binding protein (TBP)	CCCTATCACTCCTGCCACACCAGC	GTGCAATGGTCTTTAGGTCAAGTTTACAGCC
Glyceraldehyde-3-phosphate dehydrogenase (GAPDH)	AGGTCGGTGTGAACGGATTTG	TGTAGACCATGTAGTTGAGGTCA
Sirtuin 1 exon 1 (Sirt1 exon 1)	ATATATCCCGGACAGTTCCAGCCG	GGATTCCTGCAACCTGCTCCAAGG
Sirtuin 1 exon 4 (Sirt1 exon 4)	ACTTGAAGAATGGTCTTGG	CTATGCTCGCCTTGCGGTGGA
Sirtuin 2 (Sirt2)	CGCTACATGCAGAGCGAGCGCT	GTTTGCATAGAGGCCAGTGGACGG
Sirtuin 3 (Sirt3)	GTTGGCCAAGGAGCTGTACCCTGG	GCTTCAACCAGCTTTGAGGCAGG
Sirtuin 4 (Sirt4)	TTTCCTCTGAGTTCCGCTGCTCAA	AAGGCGACACAGCTACTCCATCAA
Sirtuin 5 (Sirt5)	AAACCTGGATCCTGCCATTCTGGA	TGGTCTCCATGTTAAACTCGGCCA
Sirtuin 6 (Sirt6)	GGTTCAGCTAGAACGCATGG	GTCTGCACATCACCTCATCC
Sirtuin 7 (Sirt7)	CCATGGAGCTCTGAGATGG	AAGGAAGGCCTGTGAGTGC
PPAR-γ coactivator 1α	AGCCGTGACCACTGAC	GCTGCATGGTTCTGAGT

(PGC1α)	AACGAG	GCTAAG
PPAR-γ coactivator 1β (PGC1β)	CCCAGCGTCTGACGTGGACGAGC	CCTTCAGAGCGTCAGAGCTTGCTG
PGC-related coactivator (PRC)	GGAAGACTTTGATCCTGCTCCTG	GGTTGGAAGAGGCTGGACACCTCC
Transcription factor A, mitochondrial (TFAM)	GGTATGGAGAAGGAGGCCCGGC	CGAATCATCCTTTGCCTCCTGGAAGC
Cytochrome C, somatic (CYCS)	GCAAGCATAAGACTGGACCAAA	TTGTTGGCATCTGTGTAAGAGAATC
Cytochrome C oxidase subunit 5B (Cox5b)	GCTGCATCTGTGAAGAGGACAAC	CAGCTTGTAATGGGTTCCACAGT
ATP synthase subunit O (ATP5o)	AGGCCCTTTGCCAAGCTT	TTCTCCTTAGATGCAGCAGAGTACA
NADH dehydrogenase 1β subcomplex 5 (NDUFB5)	TTTTCTCACGCGGAGCTTTC	ATAAAGAAGGCTTGACGACAAACA
Mitochondrial-encoded NADH dehydrogenase 1 (ND1)	GTGGCTCATCTACTCCACTGA	TCGAGCGATCCATAACAATAA
Mitochondrial-encoded NADH dehydrogenase 2 (ND2)	ACCCACGATCAACTGAAGC	TGTTTATAGTTGAGTACGATGGCC
Mitochondrial-encoded NADH dehydrogenase 5 (ND5)	ACCATGCTTATCCTCACTTCAG	AGTATTTGCGTCTGTTCGTCC
Cytochrome B (CytB)	CATTTATTATCGCGGCCCTA	TGTTGGGTTGTTTGATCCTG
Cytochrome C oxidase subunit I (Cox I)	CTAGCCGCAGGCATTACTAT	TGCCCAAAGAATCAGAACAG
Cytochrome C oxidase subunit II (CoxII)	GCCGACTAAATCAAGCAACA	CAATGGGCATAAAGCTATGG

Mitochondrial-encoded ATP synthase 6 (ATP6)	GACGAACATGAACCCT AAT	TACGGCTCCAGCTCATA GT
Vascular endothelial growth factor A (VEGF)	CACAGACTCGCGTTGC AAGGCGAGG	GCTGGCAGGAAGGAGCC TCCTCAGG
Carnitine palmitoyltransferase 1B (CPT1B)	GGATGTTCGAGATGCA CAGC	GGAAGCTGTAGAGCATG GGCCG
Medium-chain acyl-coenzyme A dehydrogenase (MCAD)	CAGCTAGCACTGACGC CGTGCAG	GCTCACGAGCTATGATC AGCCTCTG
Estrogen-related receptor A (ERRa)	GCCTTCTTCAAGAGGA CCATCCAG	CAGGCCTTGCGTCTCCG CTTGG
Estrogen-related receptor B (ERRb)	GCCATTGACTAAGATC GTCTCG	GCCAATTCACAGAGAGT GGTCAGG
Citrate synthase (CS)	CAGGAGGTGCTTGTCT GGCTGAC	CAGTACTGCATGACCGT ATCCTGG
Hes family BHLH transcription factor 1 (HES1)	CCAGCCAGTGTCAACA CGA	AATGCCGGGAGCTATCT TTCT

Western Blotting

Tissue and cell samples were lysed in RIPA buffer (Sigma) with Complete Mini protease inhibitor (Roche Life Science). The concentration of total protein in each lysate was measured using the BCA Assay (Life Technologies). Lysates were normalized according to total protein content and loaded onto a 4-20% Tris-Glycine Criterion Gel (Bio-Rad). Proteins were separated by polyacrylamide gel electrophoresis under denaturing conditions (SDS-PAGE) and transferred onto Immobilon PVDF membranes (Millipore, Billerica, MA). Membranes were blocked with 5% milk in TBST for 1 h at room temperature, and then incubated with the primary antibody diluted 1:1000 in 5% milk in TBST overnight at 4°C. A list of primary antibodies used in Western blotting is displayed in **Table 2**. The membranes were then washed with TBST, and

incubated with horseradish peroxidase (HRP)-conjugated species-specific secondary antibody (Jackson ImmunoResearch, West Grove, PA) diluted 1:10,000 in 5% milk in TBST buffer for 1 h at room temperature. Blots were briefly incubated with Amersham ECL chemiluminescent substrate (GE Life Sciences, Pittsburgh, PA), and chemiluminescence was recorded using high-resolution radiographic films (Denville Scientific, Holliston, MA). The integrated density of protein bands was quantified using ImageJ software (NIH, Bethesda, MD).

Table 2: Antibodies used in Western blotting

Target	Manufacturer	Catalog Number	Molecular Weight (kDa)
Sirt1	Millipore (Billerica, MA)	07-131	99-103
Acetyl-PGC1α (Lys 778)	YenZym (San Francisco, CA)	Custom	113
Total PGC1α	Millipore	ST1202	113
Acetyl-p53 (Lys 376)	Cell Signaling (Danvers, MA)	2570S	53
Total p53	Santa Cruz (Dallas, TX)	SC-126	53
NDUFB8	Abcam (Cambridge, MA)	ab110242	20
SDH8	Abcam	ab14714	30
UQCRC2	Abcam	ab14745	48
COXI	Abcam	ab14705	40
ATP5a	Abcam	ab14748	55
GAPDH	Santa Cruz	SC-265062	37
Pan-Actin	Cell Signaling	4968S	45

Immunofluorescence

Whole quadriceps muscle samples were fixed in 4% paraformaldehyde in phosphate buffered saline (PBS) (Life Technologies) overnight, embedded in paraffin wax, sectioned in the transverse plane, deposited onto glass slides, and de-paraffinized using xylenes. Antigen retrieval was performed in citrate buffer (pH 6.0). Slides were blocked in 3% bovine serum albumin (BSA) in PBST (PBS with 0.1% Triton-X) for 1 h at room temperature, and then incubated with anti-CD31 antibody (ab28364) (Abcam, Cambridge, MA) in 3% BSA in PBST overnight at 4°C. Slides were washed with PBST and then incubated with Alexa Fluor 647-conjugated secondary

antibody (Life Technologies) diluted 1:500 in 3% BSA in PBST for 1 hour at room temperature. Slides were washed again with PBST and mounted with DAPI mounting medium (Vector Labs, Burlingame, CA). Images were acquired using a confocal fluorescence microscope (Olympus, Waltham, MA) with fixed laser intensity, gain, and acquisition time. Quantification of capillaries was performed using ImageJ software (NIH) on 4 random fields chosen from the mid-portions (transitional zones) of transverse sections from quadriceps muscles. All quantifications were performed blindly.

Treadmill Endurance Testing

Treadmill endurance testing was performed using a motor-driven treadmill (TSE Systems, Chesterfield, MO). For all experiments, the treadmill was positioned at an upward incline of +15°. Mice were acclimatized to the treadmill system for 3 days prior to endurance testing. On the first day, mice were acclimatized for 10 min at 10 m/min, followed by 10 min of resting, and then another 10 min at 10 m/min. On the second and third days, mice were acclimatized for 10 min at 10/min, followed by 10 min of resting, and then another 10 min during which the speed started at 10 m/min and increased at 1 m/min every minute. The running protocol used for endurance testing was 5 min at 5 m/min (warm up), and then the speed was increased at 1/min every minute until 21 m/min, at which point speed was kept constant at 21 m/min for 20 min. After 20 min, the speed was increased to 22 m/min and held constant until mice were exhausted. Mice were considered exhausted when they sat on the shocker plate for more than 10 s without attempting to reinitiate running.

MS1 Endothelial Cell Culture and Transfection

MS1 endothelial cells were purchased from ATCC (Manassas, VA). MS1 endothelial cells were maintained in high glucose DMEM supplemented with 10% FBS, 100 IU/mL penicillin, and 100 mg/mL streptomycin at 37°C in a humidified incubator with 5% CO_2. For Sirt1 knockdown, the culture medium was replaced with Opti-MEM (Life Technologies) and MS1s were transfected with esiRNA targeting murine Sirt1 (000411, Sigma-Aldrich) using Lipofectamine 2000 (Life Technologies). For inhibition of Notch signaling, MS1s were pre-incubated with 10 μM DAPT in DMEM for 12 h prior to use in Transwell migration assays.

Scratch "Wound Healing" Assay

Upon reaching monolayer confluence, MS1 endothelial cells were serum-starved in DMEM supplemented with 0.2% FBS overnight and then scratched using a sterile P1000 pipette tip. Images were taken at the same location using a brightfield inverted microscope (Zeiss, Portland, OR) every 12 h. The area of gap closure was calculated using ImageJ software (NIH). All quantifications were performed blindly.

Transwell Migration Assay

MS1 endothelial cells were serum-starved in DMEM supplemented with 0.2% FBS overnight, and then plated at a density of 50,000 cells per insert in the upper compartment of Transwell inserts (8.0 μm pore size) (Corning Life Sciences) which had been pre-warmed with DMEM with 0.2% FBS at 37°C for 2 h. At 30 min after plating the cells, media in the lower compartment was replaced with chemoattractant media (either DMEM containing 10 ng/mL VEGF and 0.2% FBS in the presence or absence of 10 μM DAPT, or conditioned media collected from differentiated C2C12 myotubes transfected with adenoviral expression constructs for PGC1α). Migration of MS1 endothelial cells to the lower compartment of the Transwell inserts was measured after 18 h. Migrated MS1 cells were fixed with 4% paraformaldehyde in PBS for 20 min at room temperature, and cells remaining in the upper compartment were removed using cotton swabs. Transwell membranes were blocked with 5% BSA in TBST and then stained with phallioidin-FITC in TBST for 4 h to visualize filamentous actin. Transwell inserts were washed 3x in PBST and mounted onto slides with DAPI mounting medium (Vector Labs). Images were acquired using a fluorescence microscope (Olympus, Waltham, MA). Quantification of the number of migrated cells was performed using ImageJ software (NIH) on 4 random fields of each Transwell membrane. All quantifications were performed blindly.

Statistical Analysis

Data are presented as means ± standard deviations. Statistical significance was performed using the two-tailed Student's T-test. P values of less than 0.05 were considered statistically significant.

RESULTS

All data presented in this thesis were obtained directly by the author, George X. Huang.

Aim 1 Results

PGC1α activity is not suppressed by deletion of Sirt1 exon 4 in differentiated primary myoblasts

In preliminary studies, primary skeletal myoblasts were isolated from Sirt1flox mice and then differentiated into myofibers *in vitro*. Differentiated myofibers were then transduced with adenoviral overexpression vectors for Cre recombinase (or GFP) and PGC1α. No significant differences in mRNA expression of the housekeeping gene HPRT were detected among the study groups (**Figure 4A**). Deletion of Sirt1 exon 4 in cells transduced with adeno-Cre was verified by RT-qPCR (**Figure 4B**). Adenoviral-mediated overexpression of PGC1α caused robust induction of expression for genes of the TCA cycle (CS), oxidative phosphorylation (CYCS, Cox5b), fatty acid oxidation (CPT1B, MCAD), transcription factors responsive to PGC1α (ERRa, ERRb), and angiogenic factors (VEGF) (**Figures 4C-G**). Furthermore, no differences were detected between myofibers transduced with Adeno-Cre and Adeno-PGC1α and compared to myofibers transduced with Adeno-GFP and Adeno-PGC1α, indicating that Sirt1 activity is not required for activity of PGC1α in differentiated primary myoblasts.
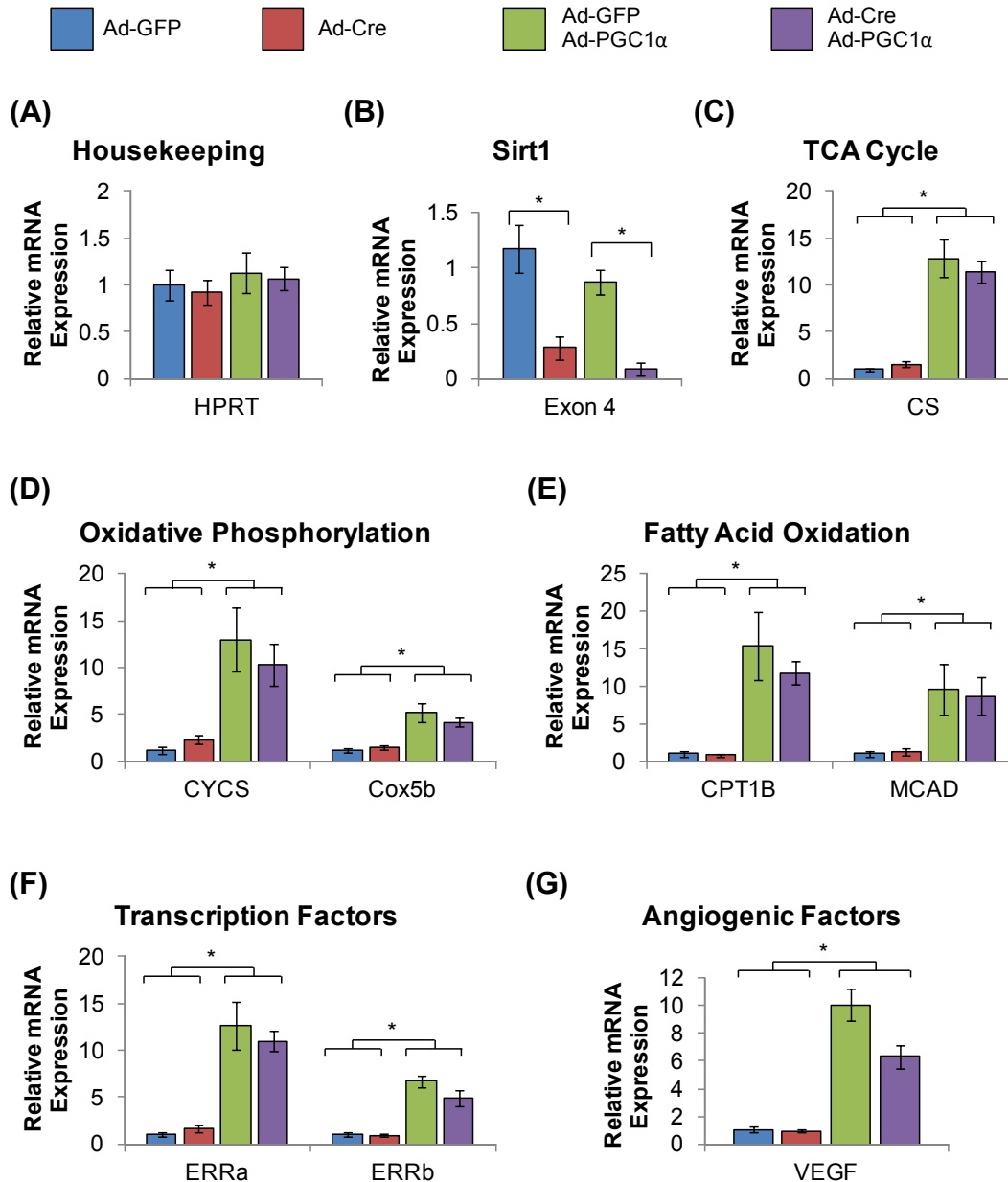
Figure 4: Deletion of Sirt1 exon 4 does not impair PGC1α activity in differentiated primary myoblasts.

Primary myoblasts were harvested from Sirt1flox mice, differentiated into myotubes, and transfected with Adeno-Cre or Adeno-GFP and then Adeno-PGC1α. mRNA was isolated from transfected cells and analyzed by RT-qPCR. The figure shows mRNA expression levels of (A) the housekeeping gene HPRT, (B) Sirt1 exon 4, (C) the TCA cycle gene CS, (D) genes of oxidative phosphorylation (CYCS and Cox5B), E) genes of fatty acid oxidation (CPT1B and MCAD), (F) transcription factors induced by PGC1α (ERRa and ERRb), and (G) the angiogenic factor VEGF. A sample size of n=4 was used for each condition. Asterisks indicate statistical significance at $p<0.05$.

Sirt1 exon 4 is deleted in skeletal myofibers of Sirt1flox Myog-Cre mice

The role of skeletal myofiber Sirt1 in regulating the activity of PGC1α was then investigated *in vivo* using mice with myofiber-specific deletion of Sirt1 exon 4. First, deletion of Sirt1 exon 4 in skeletal myofibers was confirmed at the genomic DNA (gDNA) level by qPCR analysis. In whole tibialis anterior samples, Sirt1flox Myog-Cre mice exhibited a 36.2±4.1% reduction of Sirt1 exon 4 gDNA content compared to Sirt1flox mice (**Figure 5**).
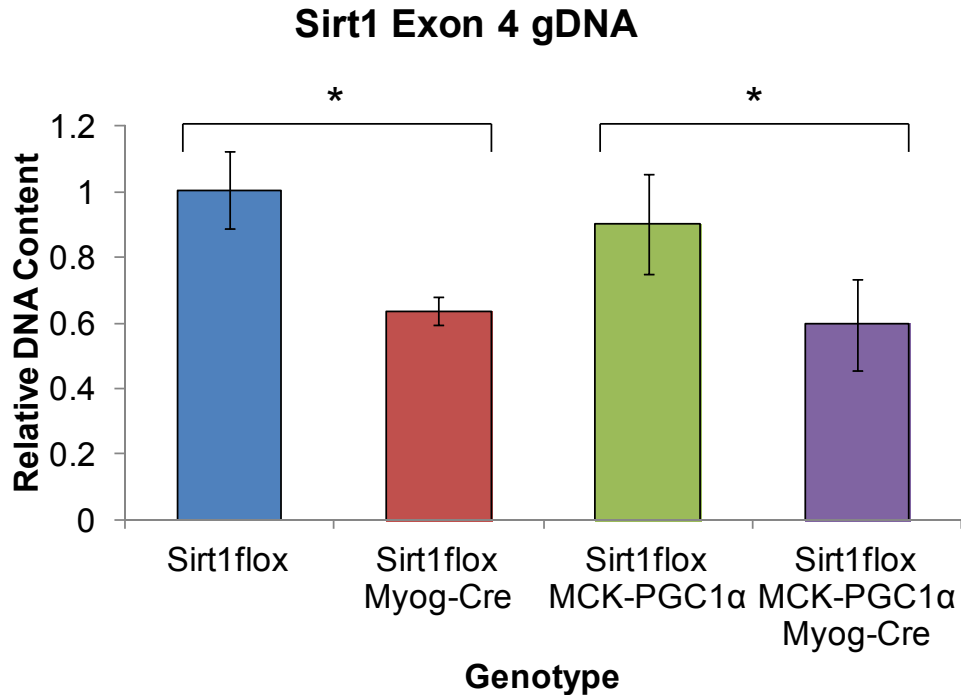
Sirt1 Exon 4 gDNA

Figure 5: Deletion of Sirt1 exon 4 in skeletal myofibers was verified at the gDNA level.

Whole quadriceps muscles were harvested from 4-month-old mice. Total gDNA was isolated from the samples and then analyzed by qPCR. Sirt1 exon 4 levels were normalized to levels of PRC as a gDNA control. Samples sizes were as follows: n=7 for Sirt1flox mice, n=4 for Sirt1flox Myog-Cre mice, n=17 for Sirt1flox MCK-PGC1α mice, and n=13 for Sirt1flox MCK-PGC1α Myog-Cre mice. Asterisks indicate statistical significance at $p<0.05$.

Deletion of Sirt1 exon 4 in skeletal myofibers was also confirmed at the mRNA level by RT-qPCR analysis. In whole quadriceps samples, no significant differences in mRNA expression of housekeeping genes were detected among the study groups (**Figure 6A**). In contrast, Sirt1flox Myog-Cre exhibited a 43.4±13.5% reduction in Sirt1 exon 4 mRNA content compared to Sirt1flox mice (**Figure 6B**). Here, no compensatory induction of gene expression of other Sirtuin members was observed in mice lacking Sirt1 activity in skeletal myofibers (**Figure 6C**), although some of the mitochondrial Sirtuins (Sirt3 and Sirt5) were induced by PGC1α overexpression as expected. Overexpression of PGC1α under the MCK promoter was also confirmed at the mRNA level by RT-qPCR analysis. In whole quadriceps samples, Sirt1flox MCK-PGC1α mice exhibited a 16.6±3.9-fold increase in mRNA for PGC1α, compared to Sirt1flox mice (**Figure 6D**). Here, no compensatory induction of gene expression of other

members of the PGC1 family (PGC1β and PRC) was observed in mice lacking Sirt1 activity in skeletal myofibers (**Figure 6E**).
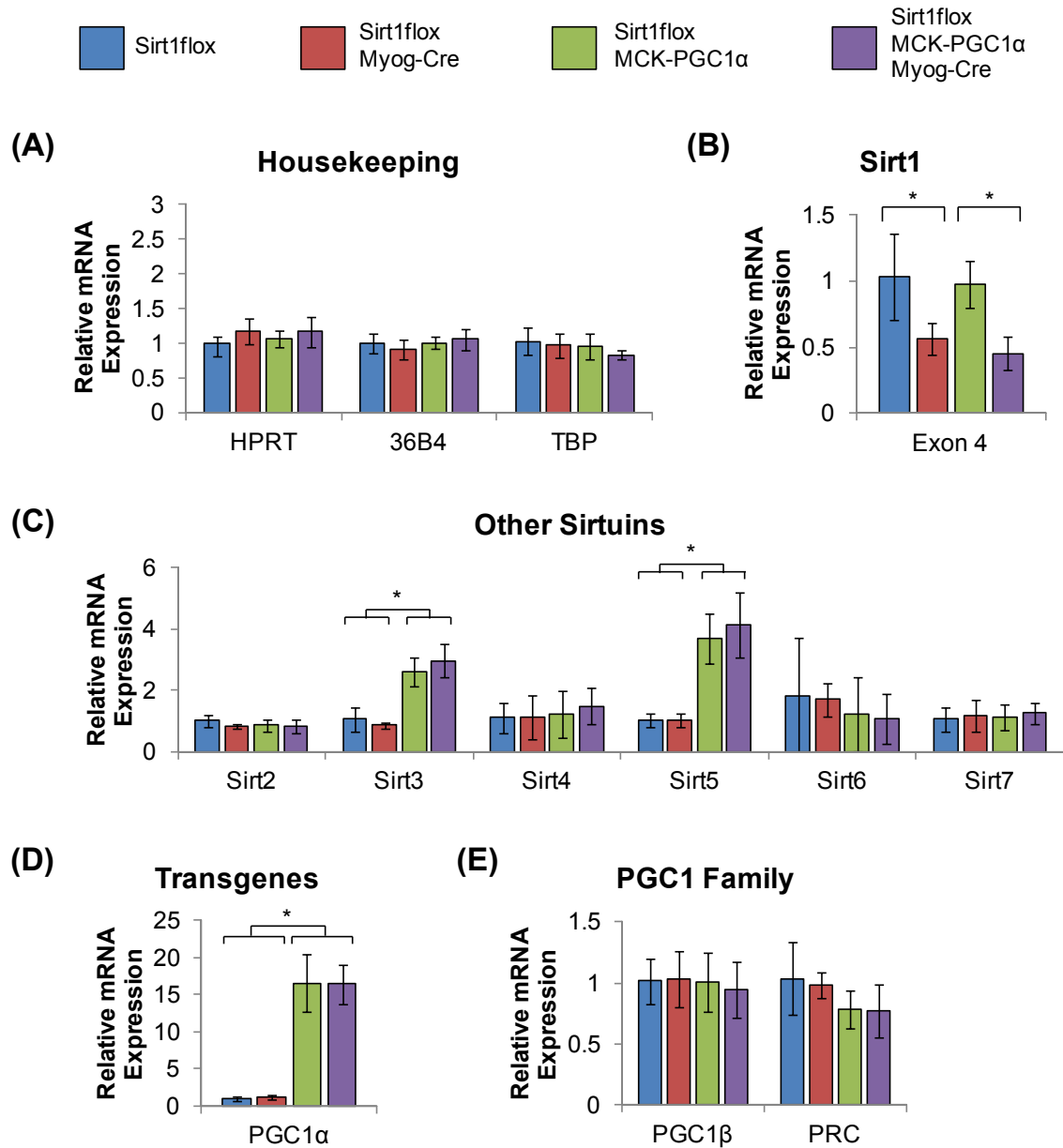
Figure 6: Deletion of Sirt1 exon 4 in skeletal myofibers was verified at the mRNA level.

Whole quadriceps muscles were harvested from 4-month-old mice. Total mRNA was isolated from the samples and then analyzed by RT-qPCR. (A) mRNA expression levels of housekeeping genes (HRPT, 36B4, and TBP). (B) mRNA expression levels of Sirt1 exon 4. (C) mRNA expression levels of Sirtuins 2-7. (D) mRNA expression mRNA expression levels of PGC1α. (D) mRNA expression levels of other members of the PGC1 family (PGC1β and PRC). Sample sizes were as follows: n=4 for Sirt1flox mice, n=4 for Sirt1flox Myog-Cre mice, n=12 for Sirt1flox MCK-PGC1α mice, and n=13 for Sirt1flox MCK-PGC1α Myog-Cre mice. Asterisks indicate statistical significance at p<0.05.

Finally, deletion of Sirt1 exon 4 in skeletal myofibers was confirmed at the protein level by Western blotting. In whole quadriceps lysates from Sirt1flox Myog-Cre mice, a shortened variant (ΔExon 4) of the Sirt1 protein which migrated at ~99 kDa was detected in addition to the wildtype Sirt1 protein which migrated at ~103 kDa (**Figure 7A**). Upon quantification by densitometry, the intensity of the ΔExon 4 bands in lysates from Sirt1flox Myog-Cre mice represented 49.2±7.4% of the total intensity of the Sirt1 bands, indicating that Sirt1 exon 4 was efficiently deleted in skeletal myofibers. In contrast, only the wildtype Sirt1 protein was detected in quadriceps lysates from Sirt1flox mice (**Figure 7A**).

Furthermore, as a reporter assay for loss of Sirt1 catalytic activity, the acetylation status of p53 was assessed by Western blotting using an antibody specific for the acetylated protein (acetylated at Lys376). The amount of total p53 was unchanged between quadriceps lysates from Sirt1flox mice and Sirt1flox Myog-Cre mice. However, the level of acetylated p53 was on average 77.6% higher in lysates from Sirt1flox Myog-Cre mice compared to Sirt1flox mice (**Figures 7A and B**), thus confirming the loss of Sirt1 activity in skeletal myofibers in Sirt1flox Myog-Cre mice.

The acetylation status of PGC1α at baseline (i.e. in mice that do not overexpress PGC1α) was also evaluated by Western blotting using an antibody specific for acetylated PGC1α (acetylated at Lys778). The level of acetylated PGC1α was on average slightly (23.4%) higher in lysates from Sirt1flox Myog-Cre mice compared to Sirt1flox mice, however this difference was not statistically significant (**Figures 7A and B**), indicating that deacetylation of PGC1α at Lys778 was unchanged at baseline despite loss of Sirt1 catalytic activity in skeletal myofibers.

(A)

(B)
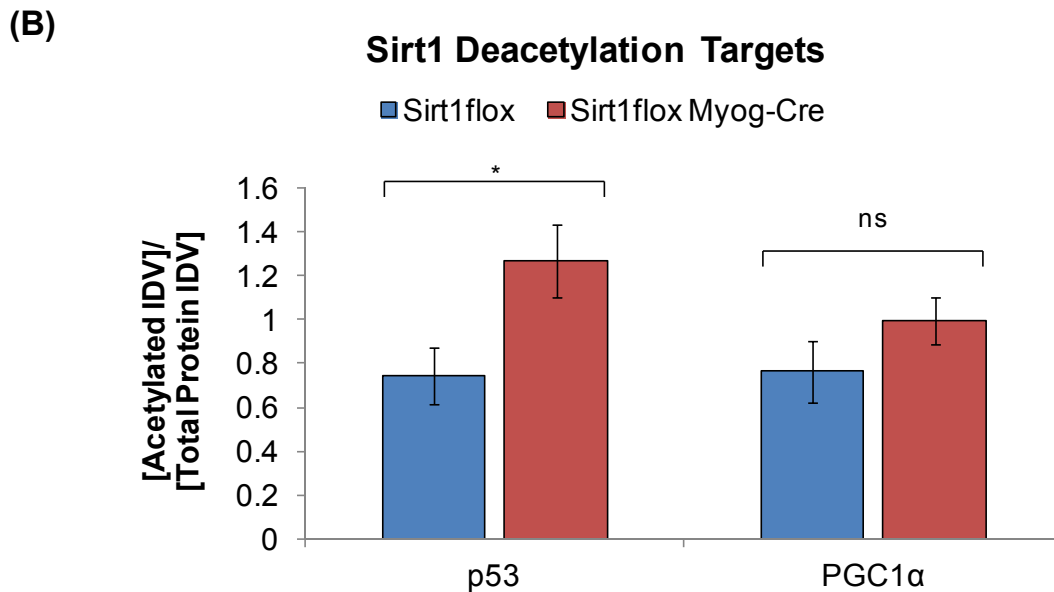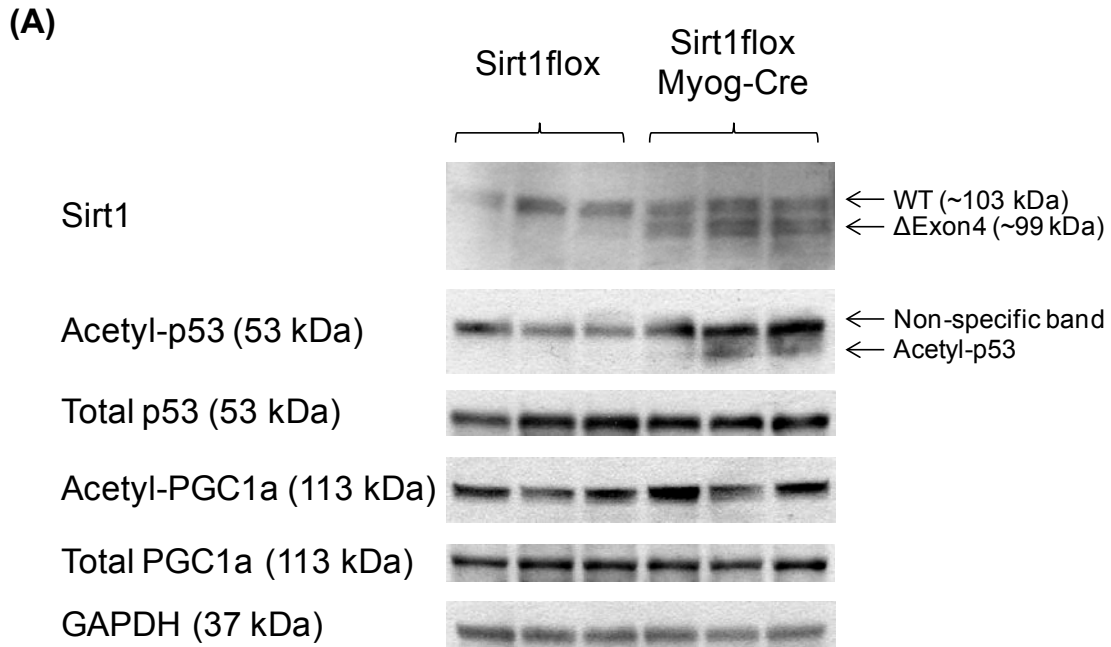
Figure 7: Deletion of Sirt1 exon 4 in skeletal myofibers was verified at the protein and catalytic activity levels.

Whole quadriceps muscles were harvested from 4-month-old mice and lysed for analysis by Western blotting. (A) Western blots showing protein levels of Sirt1, acetylated PGC1α (Lys778), Total PGC1α, acetylated p53 (Lys376), and total p53. The Sirt1 variant lacking exon 4 migrates faster (~99 kDa) than the wildtype Sirt1 protein (~103 kDa). GAPDH was used as a loading control. (B) Quantification of integrated band density (IDV) (n=3 for each genotype). Asterisks indicate statistical significance at $p < 0.05$.

PGC1α activity is not suppressed by deletion of Sirt1 exon 4 in skeletal myofibers

Upon confirmation that Sirt1 exon 4 was deleted from skeletal myofibers at the gDNA, mRNA, protein, and enzymatic activity levels, the activity of overexpressed PGC1α was evaluated in these mice.

The activity of PGC1α was first evaluated by examining its ability to induce expression of genes involved in oxidative metabolism. Specifically, the levels of mRNA transcripts for numerous genes responsive to PGC1α – including nuclear-encoded genes (TFAM, CYCS, Cox5b, ATP5o, NDUFB5), mitochondrial-encoded genes (ND1, ND2, ND5, CytB, Cox I, Cox II, ATP6), and angiogenic factors (VEGF) – were measured by RT-qPCR. As described above, no significant differences in mRNA expression of housekeeping genes were detected in quadriceps samples from the study groups (**Figure 6A**). Overexpression of PGC1α resulted in robust induction of expression of PGC1α-responsive genes in samples from Sirt1flox MCK-PGC1α mice (**Figures 8A-C**). Notably, induction of all of these genes was preserved in quadriceps samples from Sirt1flox MCK-PGC1α Myog-Cre mice as compared to samples from Sirt1flox MCK-PGC1α mice (**Figures 8A-C**), indicating that PGC1α activity remained intact in skeletal myofibers lacking Sirt1 catalytic activity.
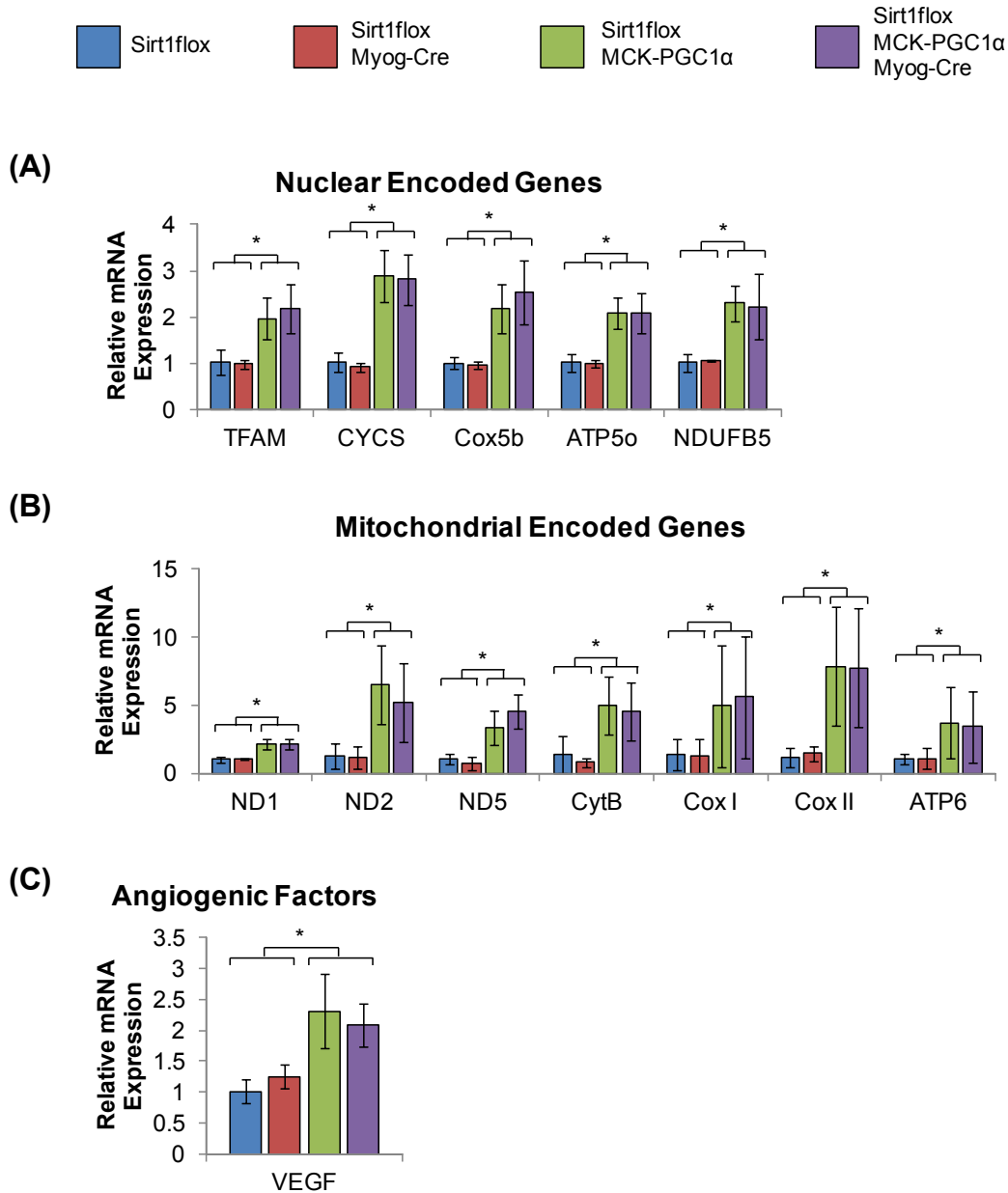
Figure 8: Knockout of Sirt1 in skeletal myofibers does not impair the ability of PGC1α overexpression to upregulate genes of oxidative metabolism and angiogenic factors.

Whole quadriceps muscles were harvested from 4-month-old mice. Total mRNA was isolated from the samples and then analyzed by RT-qPCR. (A) mRNA expression levels of nuclear encoded genes of oxidative metabolism (TFAM, CYCS, Cox5b, ATP5o, and NDUFB5). (B) mRNA expression levels of mitochondrial encoded genes of oxidative metabolism (ND1, ND2, ND5, CytB, Cox I, Cox II, and ATP6). (C) mRNA expression levels of the angiogenic factor VEGF. Sample sizes were as follows: n=4 for Sirt1flox mice, n=4 for Sirt1flox Myog-Cre mice, n=12 for Sirt1flox MCK-PGC1α mice, and n=13 for Sirt1flox MCK-PGC1α Myog-Cre mice. Asterisks indicate statistical significance at $p < 0.05$.

36

Next, the activity of PGC1α was evaluated by examining its ability to induce proteins of oxidative phosphorylation. Specifically, levels of protein from each of the oxidative phosphorylation complexes (NDUFB8 for complex I, SDH8 for complex II, UQCRC2 for complex III, COXI for complex IV, and ATP5a for Complex V) were studied by Western blotting. Upon densitometry, Sirt1flox MCK-PGC1α mice exhibited on average 4.6-fold greater levels of PGC1α protein in whole quadriceps lysates than Sirt1flox mice (**Figure 9**). In conjunction, lysates from Sirt1flox MCK-PGC1α mice had increased levels of oxidative phosphorylation proteins compared to lysates from Sirt1flox mice, indicating that PGC1α overexpression resulted in induction of oxidative phosphorylation at the protein level (**Figure 9**). Analogous to the mRNA studies, no significant differences were found in levels of oxidative phosphorylation proteins between lysates from Sirt1flox MCK-PGC1α Myog-Cre mice and Sirt1flox MCK-PGC1α mice (**Figure 9**), further underscoring that PGC1α activity remains intact in skeletal myofibers lacking Sirt1 catalytic activity.

(A)

(B)
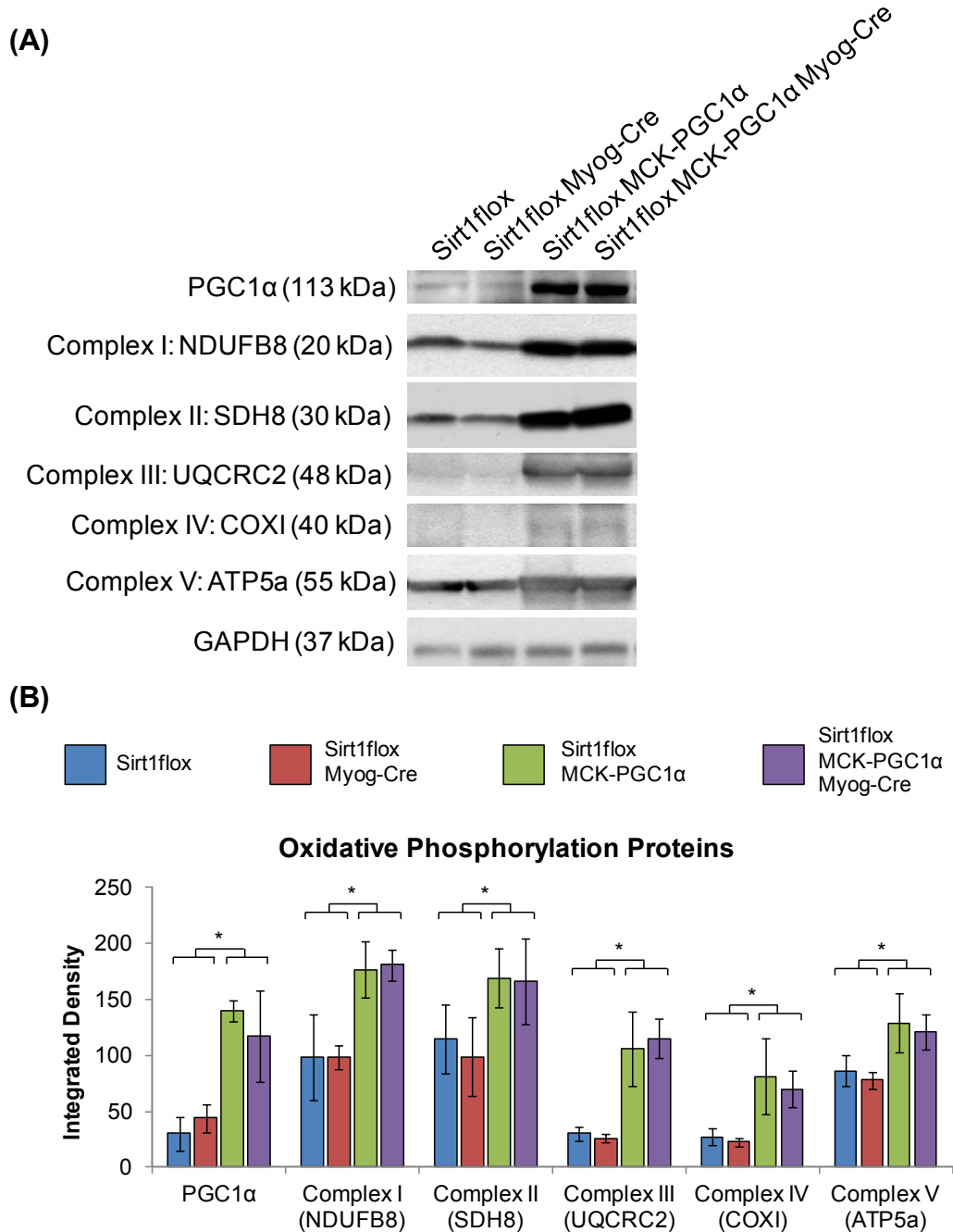
Figure 9: Knockout of Sirt1 in skeletal myofibers does not impair the ability of PGC1α overexpression to upregulate proteins of oxidative phosphorylation.

Whole quadriceps muscles were harvested from 4-month-old mice and lysed for analysis by Western blotting. (A) Representative Western blots showing protein levels of PGC1α, NDUFB5 (complex I), SDH8 (complex II), UQCRC2 (complex III), COX I (complex IV), and ATP5a (complex V). GAPDH was used as a loading control. (B) Quantification of integrated band density (n=4 for each genotype). Asterisks indicate statistical significance at p<0.05.

The cross-sectional vascular density of skeletal muscle was also examined as an output of *in vivo* PGC1α activity. Muscle cross-sections were stained for CD31, a marker of vascular endothelium, and capillary density was quantified at the transitional zone of the quadriceps muscle. Quadriceps from Sirt1flox MCK-PGC1α mice exhibited on average a 121.2% increase in capillary density compared to Sirt1flox mice, and quadriceps from Sirt1flox MCK-PGC1α Myog-Cre mice exhibited similar vascular density to those from Sirt1flox MCK-PGC1α mice (**Figures 10A and B**).

(A)

| | Sirt1flox | Sirt1flox Myog-Cre | Sirt1flox MCK-PGC1α | Sirt1flox MCK-PGC1α Myog-Cre |

DAPI

CD31

Merged

(B)

Capillaries per HPF

Capillary Density per HPF
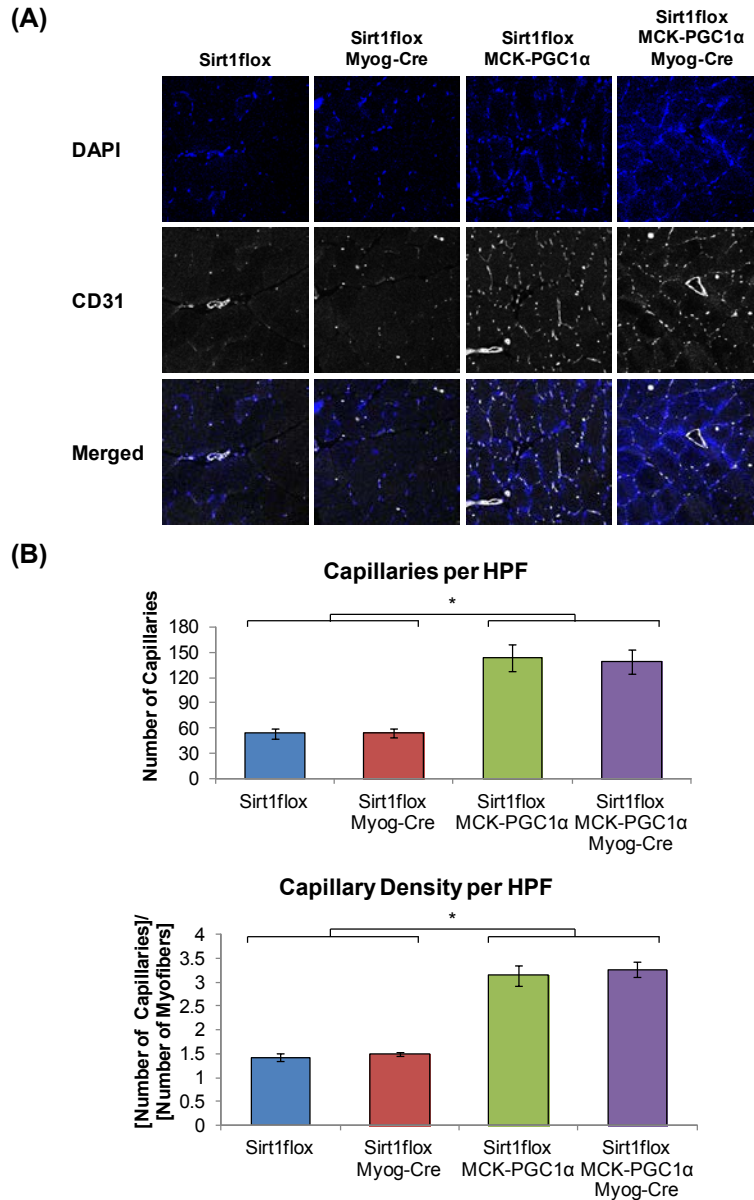
Figure 10: Knockout of Sirt1 in skeletal myofibers does not impair the ability of PGC1α overexpression to increase vascular density in skeletal muscle tissue.

Whole quadriceps muscles were harvested from 4-month-old mice, fixed, and processed for histological analysis. Muscle cross-sections were stained using an antibody to CD31 (a marker of vascular endothelium) and DAPI. Images were taken at the transitional zones of the quadriceps muscle group. (A) Representative images of CD31 and DAPI immunofluorescence from muscle cross-sections. (B) Quantification of vascular density, reported as the number of capillaries per high power field (upper panel) and the number of capillaries per myofiber (lower panel). Sample sizes were as follows: n=6 for Sirt1flox mice, n=3 for Sirt1flox Myog-Cre mice, n=10 for Sirt1flox MCK-PGC1α mice, and n=5 for Sirt1flox MCK-PGC1α Myog-Cre mice. Asterisks indicate statistical significance at $p < 0.05$.

Finally, the forced exercise endurance capacity was examined in these mice using treadmill testing. Sirt1flox MCK-PGC1α mice ran on average for 2.3x the distance and 2.0x the duration of Sirt1flox mice (**Figure 11**). Although Sirt1flox MCK-PGC1α Myog-Cre mice exhibited slightly less endurance capacity than Sirt1flox MCK-PGC1α mice (**Figure 11**), these differences mice were not statistically significant.

Thus, knockout of Sirt1 in skeletal myofibers did not impair the ability of PGC1α overexpression to upregulate transcripts of oxidative metabolism and proteins of oxidative phosphorylation, to increase vascular density in skeletal muscle, or to enhance treadmill endurance capacity *in vivo*.
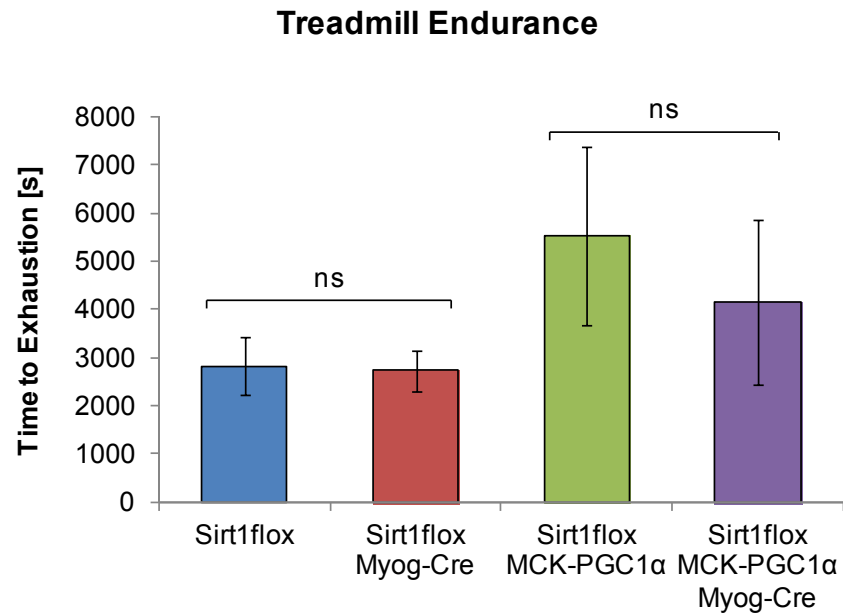
(A)

Treadmill Endurance

(B)

Treadmill Endurance
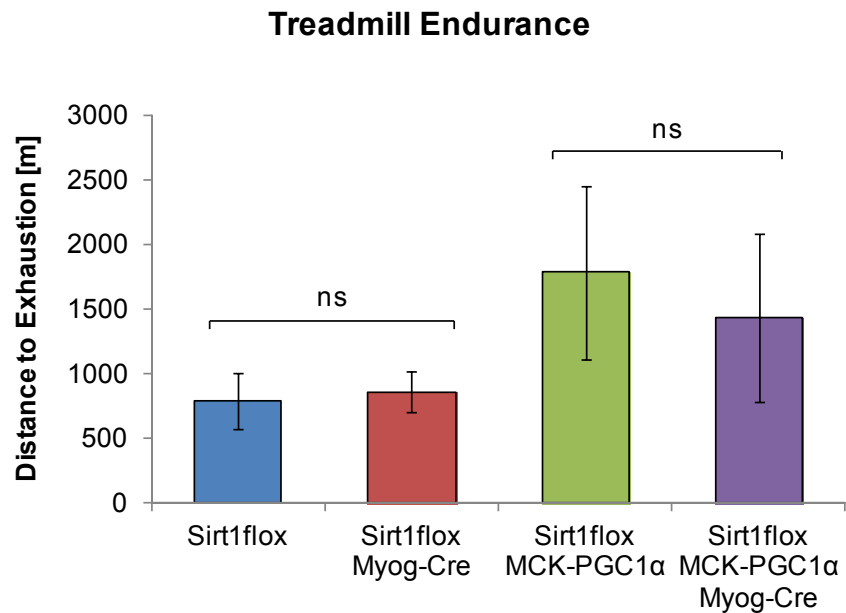
Figure 11: Knockout of Sirt1 in skeletal myofibers does not impair the ability of PGC1α overexpression to increase treadmill endurance.

4-month-old mice were acclimatized to a rodent treadmill and then subjected to a forced treadmill endurance testing protocol. Exhaustion was defined as the endpoint when each subject rested on the shocker plate for 10 s continuously. (A) Time elapsed until exhaustion. (B) Distance run until exhaustion. Sample sizes were as follows: n=7 for Sirt1flox mice, n=4 for Sirt1flox Myog-Cre mice, n=7 for Sirt1flox MCK-PGC1α mice, and n=4 for Sirt1flox MCK-PGC1α Myog-Cre mice.

Aim 2 Results

Next, the role of endothelial Sirt1 in coordinating adaptations of skeletal muscle in response to PGC1α overexpression was investigated *in vivo*.

Sirt1 exon 4 is deleted in endothelial cells of Sirt1flox Tie2-Cre mice.

First, deletion of Sirt1 exon 4 in the endothelium was confirmed at the genomic DNA level by qPCR analysis. In whole tibialis anterior samples, Sirt1flox Tie2-Cre mice exhibited a 45.7±1.5% reduction of Sirt1 exon 4 gDNA content compared to Sirt1flox mice (**Figure 12**).
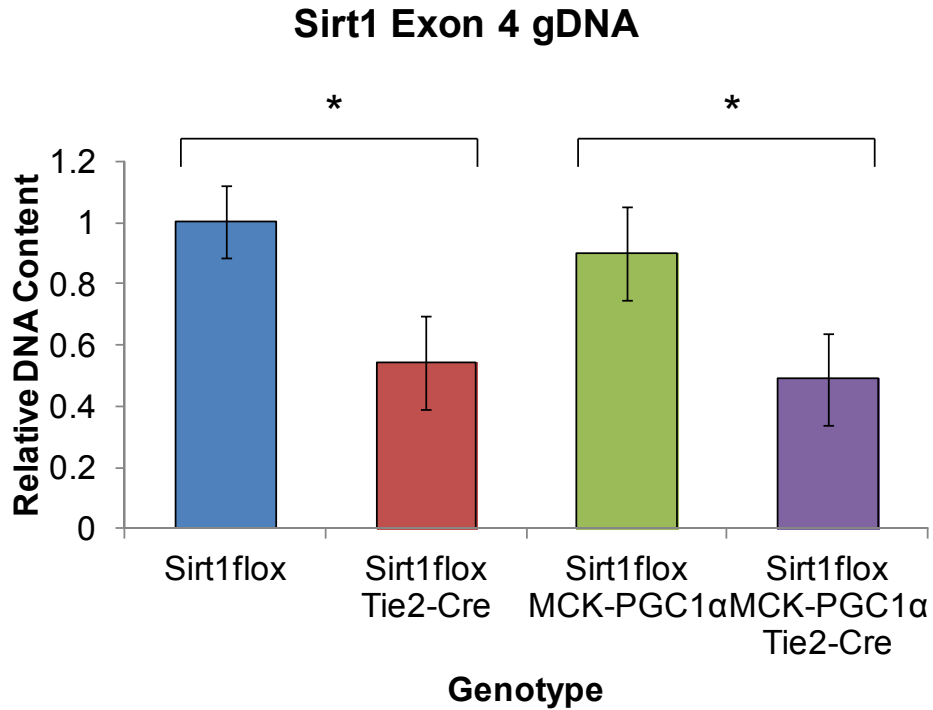
Sirt1 Exon 4 gDNA

Figure 12: Deletion of Sirt1 exon 4 in the endothelium was verified at the gDNA level.

Whole quadriceps muscles were harvested from 4-month-old mice. Total gDNA was isolated from the samples and then analyzed by qPCR. Sirt1 exon 4 levels were normalized to levels of PRC as a gDNA control. Samples sizes were as follows: n=7 for Sirt1flox mice, n=4 for Sirt1flox Tie2-Cre mice, n=17 for Sirt1flox MCK-PGC1α mice, and n=5 for Sirt1flox MCK-PGC1α Tie2-Cre mice. Asterisks indicate statistical significance at p<0.05.

Deletion of Sirt1 exon 4 in endothelial cells was also confirmed at the mRNA level by RT-qPCR analysis. While deletion of Sirt1 exon 4 in the endothelium was not detected at the mRNA level in whole quadriceps samples (**Figure 13E**), detection was possible using whole lung samples, which have a relatively higher density of endothelial cells compared to skeletal muscle. Here, no significant differences in mRNA expression of housekeeping genes were detected among the study groups (**Figure 13A**), but lung tissue from Sirt1flox Tie2-Cre mice exhibited a 50.9±21.8% reduction in Sirt1 exon 4 mRNA content compared to lung tissue from Sirt1flox mice (**Figure 13B**). Again, no compensatory induction of gene expression of other Sirtuins was observed in mice lacking Sirt1 activity in the endothelium (**Figure 13C**). Overexpression of PGC1α under the MCK promoter was also confirmed at the mRNA level by RT-qPCR analysis of whole quadriceps samples. While no significant differences in mRNA

expression of housekeeping genes was detected among the study groups (**Figure 13D**), Sirt1flox MCK-PGC1α mice exhibited a 10.8±4.6-fold increase in mRNA for PGC1α, compared to Sirt1flox mice (**Figure 13F**). Furthermore, no compensatory induction of gene expression of other members of the PGC1 family was observed in mice lacking Sirt1 activity in endothelial cells (**Figure 13G**).
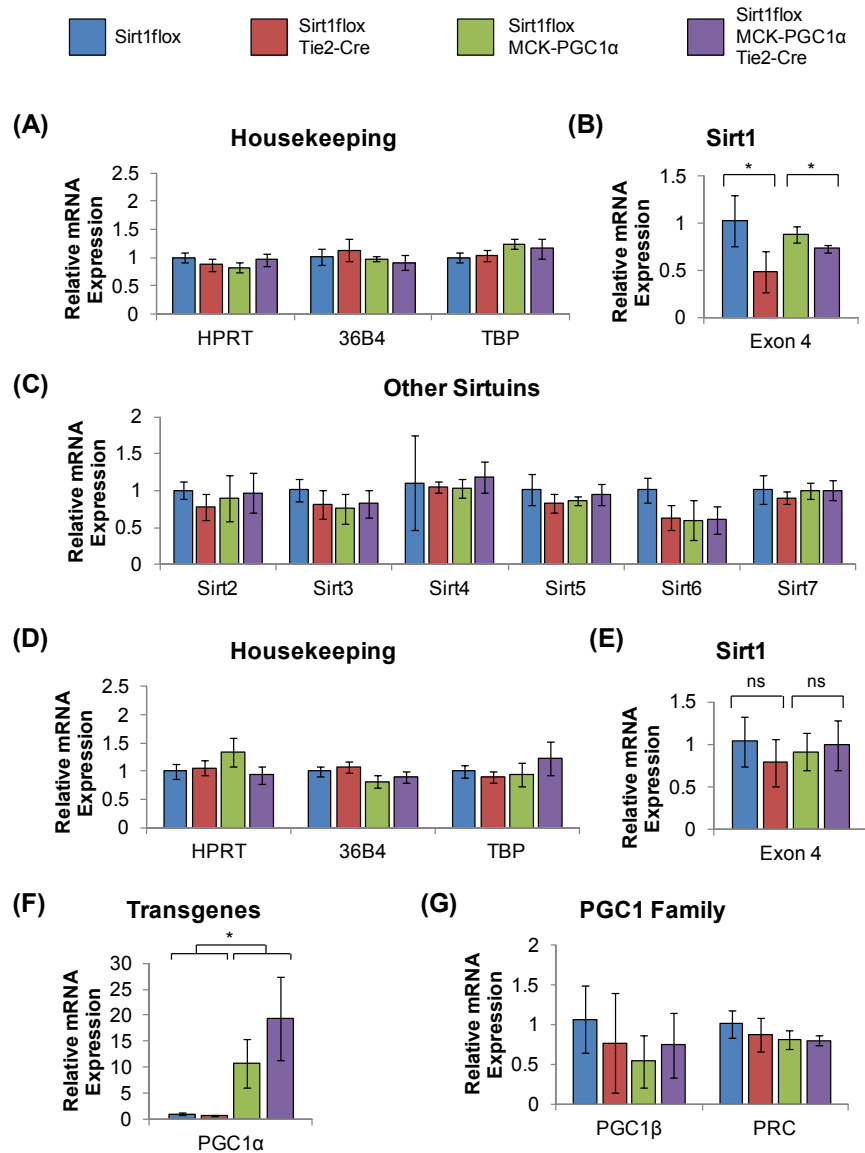
Figure 13: Deletion of Sirt1 exon 4 in the endothelium was verified at the mRNA level.

Whole lung samples (A-C) and whole quadriceps samples (D-F) were harvested from 4-month-old mice. Total mRNA was isolated from the samples and then analyzed by RT-qPCR. (A) mRNA expression levels of housekeeping genes (HPRT, 36B4, and TBP) in lung samples. (B) mRNA expression levels of Sirt1 exon 4 in lung samples. (C) mRNA expression levels of Sirtuins 2-7 in lung samples. (D) mRNA expression levels of housekeeping genes (HPRT, 36B4, and TBP) in quadriceps samples. (E) mRNA expression levels of Sirt1 exon 4 in quadriceps samples. (F) mRNA expression levels of PGC1α in quadriceps samples. (G) mRNA expression levels of other members of the PGC1 family (PGC1β and PRC) in quadriceps samples. Sample sizes were as follows: n=4 for all lung samples from each genotype, n=7 for Sirt1flox quadriceps, n=4 for Sirt1flox Tie2-Cre quadriceps, n=9 for Sirt1flox MCK-PGC1α quadriceps, and n=5 for Sirt1flox MCK-PGC1α Tie2-Cre quadriceps samples. Asterisks indicate statistical significance at $p < 0.05$.

Finally, deletion of Sirt1 exon 4 in endothelial cells was confirmed at the protein level by Western blotting. In whole lung lysates from Sirt1flox Tie2-Cre mice, the shortened variant (ΔExon 4) of the Sirt1 protein was detected in addition to the wildtype Sirt1 protein (**Figure 14**). Upon quantification by densitometry, the intensity of the ΔExon 4 bands in lysates from Sirt1flox Tie2-Cre mice represented 60.9±18.4% of the total intensity of the Sirt1 bands, indicating that Sirt1 exon 4 was efficiently deleted in the endothelium. As expected, only the wildtype Sirt1 band was detected in lung lysates from Sirt1flox mice.
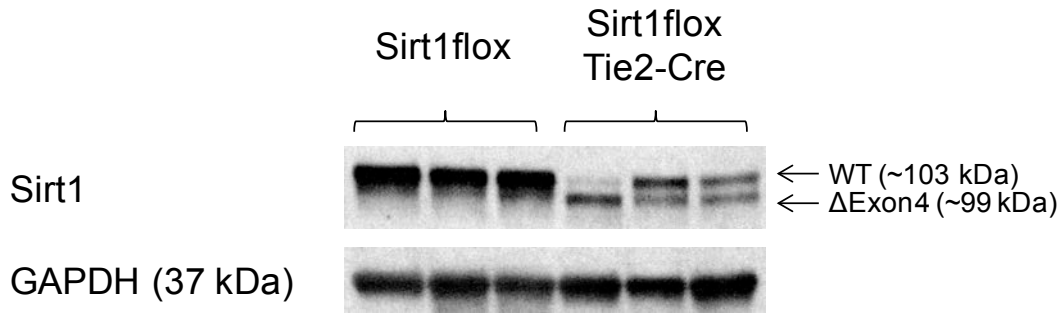
Figure 14: Deletion of Sirt1 exon 4 in the endothelium was verified at the protein level.

Whole lung samples were harvested from 4-month-old mice and lysed for analysis by Western blotting for Sirt1. The Sirt1 variant lacking exon 4 migrates faster (~99 kDa) than the wildtype Sirt1 protein (~103 kDa). GAPDH was used as a loading control.

PGC1α activity is not suppressed by deletion of Sirt1 exon 4 in endothelial cells

Upon confirmation that Sirt1 exon 4 was deleted from endothelial cells at the gDNA, mRNA, and protein levels, the adaptations of skeletal muscle tissue in response to PGC1α overexpression were evaluated in these mice.

As previously, the levels of mRNA transcripts for numerous genes responsive to PGC1α were measured by RT-qPCR. As described above, no significant differences in mRNA expression of housekeeping genes were detected in quadriceps samples from the study groups (**Figure 13D**). Overexpression of PGC1α resulted in robust induction of expression of PGC1α-responsive genes in samples from Sirt1flox MCK-PGC1α mice (**Figures 15A and B**). Notably, induction of all of these genes was preserved in quadriceps samples from Sirt1flox MCK-PGC1α Tie2-Cre mice as compared to samples from Sirt1flox MCK-PGC1α mice (**Figures 15A and B**).
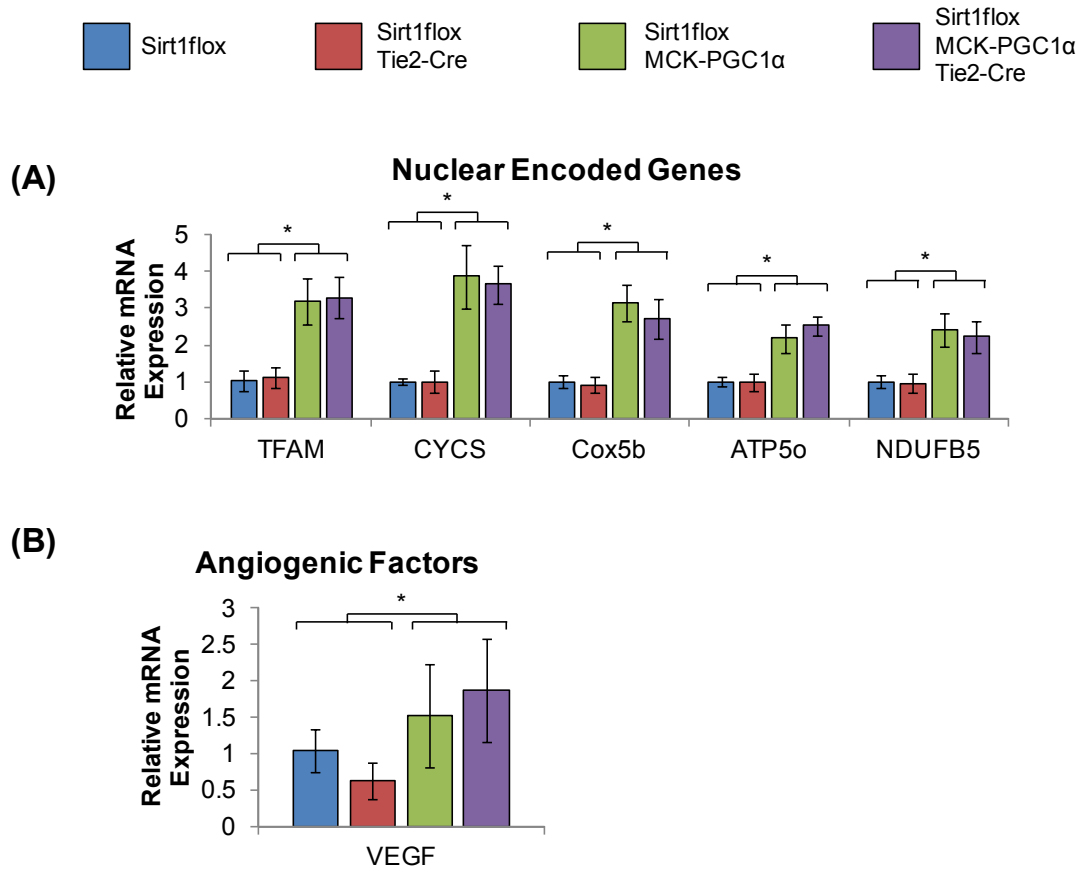
Figure 15: Knockout of Sirt1 in the endothelium does not impair the ability of PGC1α overexpression to upregulate genes of oxidative metabolism and angiogenic factors.

Whole quadriceps muscles were harvested from 4-month-old mice. Total mRNA was isolated from the samples and then analyzed by RT-qPCR. (A) mRNA expression levels of genes of oxidative metabolism (TFAM, CYCS, Cox5b, ATP5o, and NDUFB5). (B) mRNA expression levels of the angiogenic factor VEGF. Sample sizes were as follows: n=7 for Sirt1flox mice, n=4 for Sirt1flox Tie2-Cre mice, n=9 for Sirt1flox MCK-PGC1α mice, and n=5 for Sirt1flox MCK-PGC1α Tie2-Cre mice. Asterisks indicate statistical significance at p<0.05.

Upon Western blotting of whole quadriceps lysates, Sirt1flox MCK-PGC1α mice exhibited on average 2.7-fold greater levels of PGC1α protein than Sirt1flox mice (**Figure 16**) and, as expected, Sirt1flox MCK-PGC1α mice exhibited increased levels of oxidative phosphorylation proteins compared to Sirt1flox mice. Analogous to the mRNA studies, no significant differences were found in the levels of any proteins of oxidative phosphorylation between lysates from Sirt1flox MCK-PGC1α Tie2-Cre mice and Sirt1flox MCK-PGC1α mice (**Figure 16**).

(A)
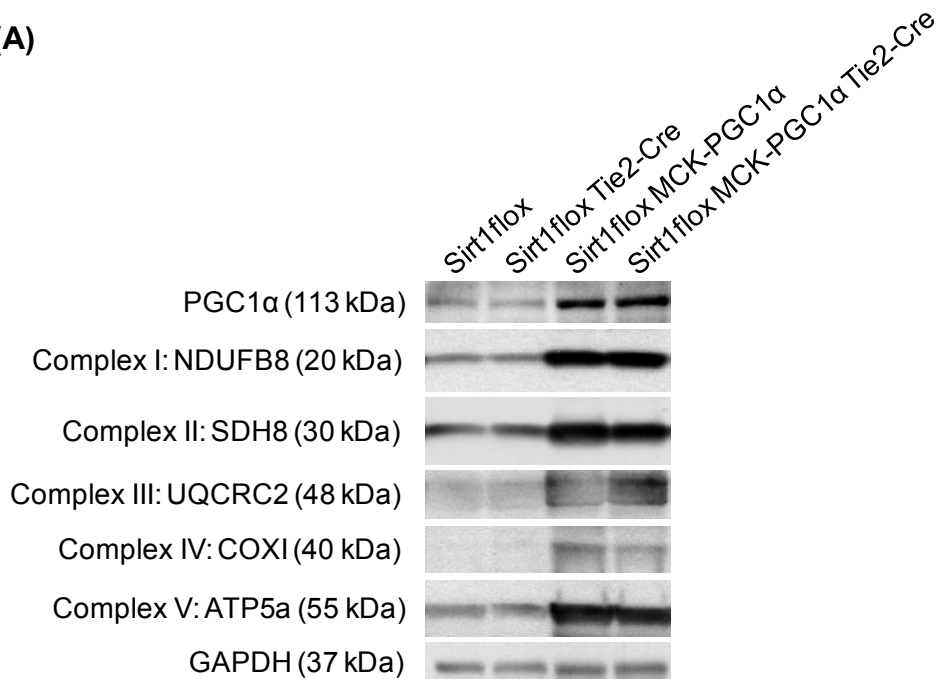
(B)
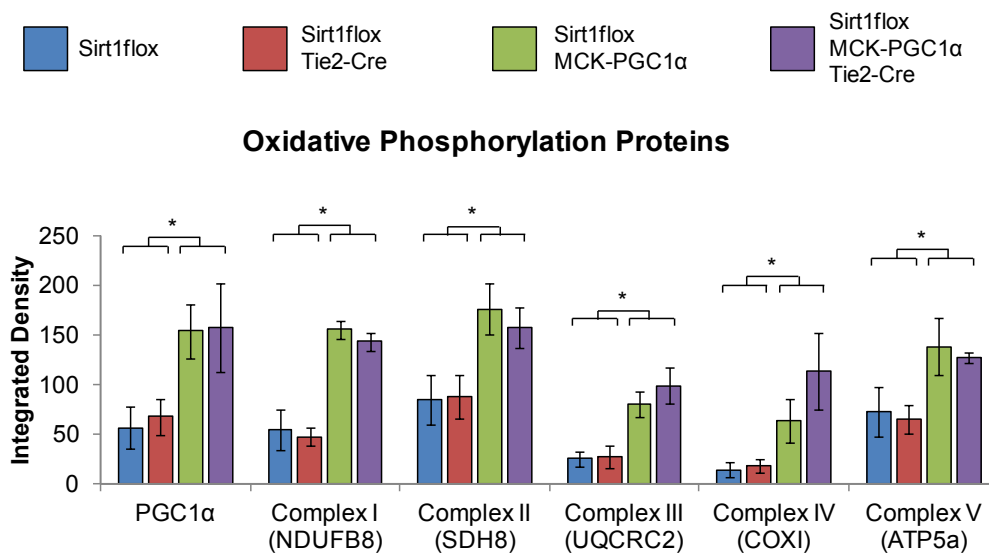
Figure 16: Knockout of Sirt1 in the endothelium does not impair the ability of PGC1α overexpression to upregulate proteins of oxidative phosphorylation.

Whole quadriceps muscles were harvested from 4-month-old mice and lysed for analysis by Western blotting. (A) Representative Western blots showing protein levels of PGC1α, NDUFB5 (complex I), SDH8 (complex II), UQCRC2 (complex III), COX I (complex IV), and ATP5a (complex V). GAPDH was used as a loading control. (B) Quantification of integrated band density (n=4 for each genotype). Asterisks indicate statistical significance at $p < 0.05$.

Angiogenesis in response to PGC1α overexpression is impaired by deletion of Sirt1 exon 4
in endothelial cells

As previously, muscle cross-sections were stained for CD31 and capillary density was quantified at the transitional zones of the quadriceps muscle. Here, although no significant differences in vascular density were detected between samples from Sirt1flox and Sirt1flox Tie2-Cre mice, Sirt1flox MCK-PGC1α Tie2-Cre exhibited significantly decreased vascular density in comparison to Sirt1flox MCK-PGC1α mice (**Figure 17**). Thus, angiogenesis in skeletal muscle tissue in response to PGC1α overexpression was impaired in mice lacking Sirt1 activity in the endothelium.
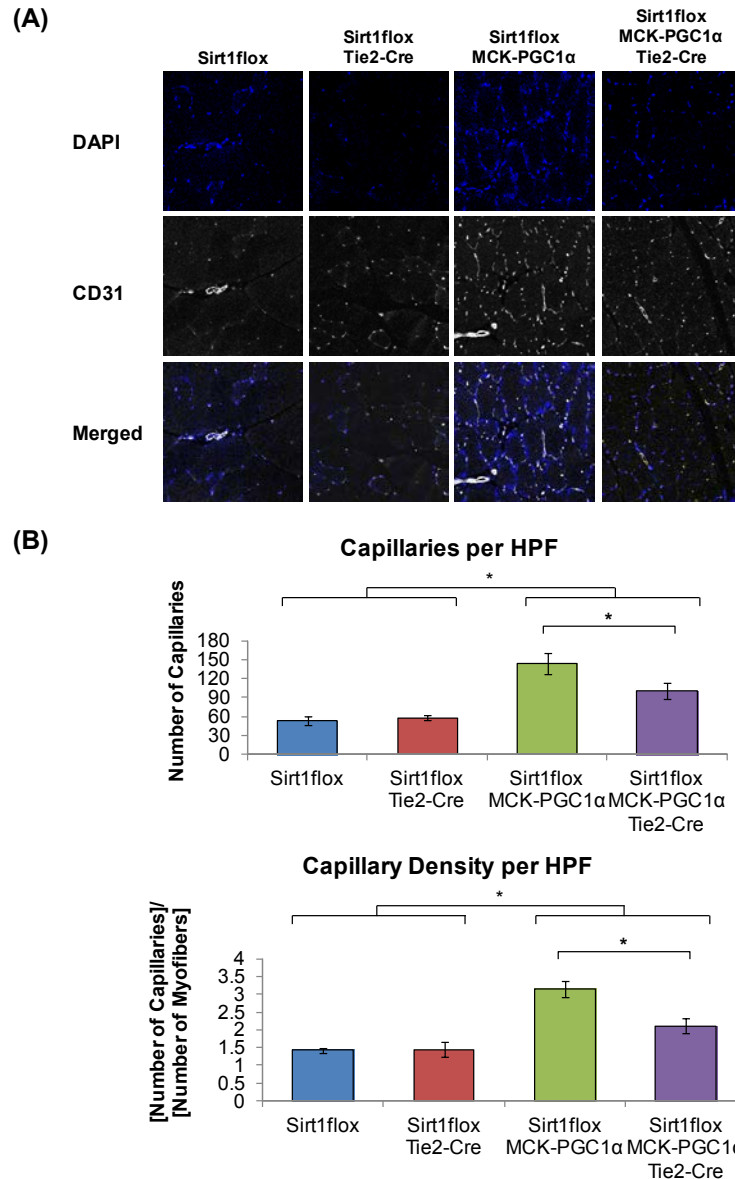
Figure 17: Knockout of Sirt1 in the endothelium impairs the ability of PGC1α overexpression to increase vascular density in skeletal muscle tissue.

Whole quadriceps muscles were harvested from 4-month-old mice, fixed, and processed for histological analysis. Muscle cross-sections were stained using an antibody to CD31 (a marker of vascular endothelium) and DAPI. Images were taken at the transitional zones of the quadriceps muscle group. (A) Representative images of CD31 and DAPI immunofluorescence from muscle cross-sections. (B) Quantification of vascular density, reported as the number of capillaries per high power field (upper panel) and the number of capillaries per myofiber (lower panel). Sample sizes were as follows: n=6 for Sirt1flox mice, n=3 for Sirt1flox Tie2-Cre mice, n=10 for Sirt1flox MCK-PGC1α mice, and n=5 for Sirt1flox MCK-PGC1α Tie2-Cre mice. Asterisks indicate statistical significance at $p < 0.05$.

Finally, the forced exercise endurance capacity was examined in these mice using treadmill testing. Sirt1flox MCK-PGC1α mice ran on average for 2.3x the distance and 2.0x the duration of Sirt1flox mice (**Figure 18**). Interestingly, Sirt1flox MCK-PGC1α Tie2-Cre mice exhibited significantly decreased treadmill endurance compared to Sirt1flox MCK-PGC1α mice (**Figure 18**), indicating that endothelial Sirt1 is also required for upregulation of endurance capacity in response to PGC1α overexpression.

In summary, although knockout of endothelial Sirt1 activity did not impair the ability of PGC1α overexpression to upregulate genes of oxidative metabolism and proteins of oxidative phosphorylation in response to PGC1α, endothelial Sirt1 activity was required for angiogenesis in skeletal muscle tissue and enhancement of treadmill endurance in response to PGC1α overexpression.

(A)

Treadmill Endurance

(B)

Treadmill Endurance
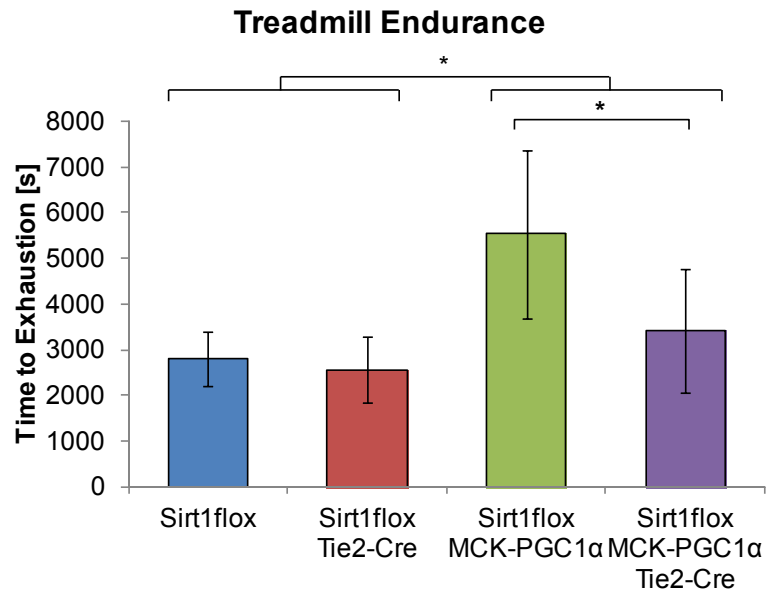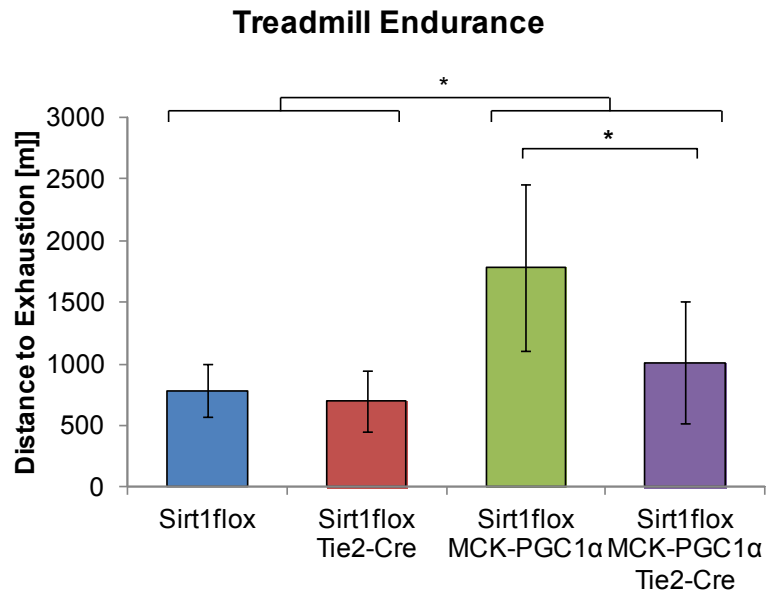
Figure 18: Knockout of Sirt1 in the endothelium impairs the ability of PGC1α overexpression to increase treadmill endurance.

4-month-old mice were acclimatized to a rodent treadmill and then subjected to a forced treadmill endurance testing protocol. Exhaustion was defined as the endpoint when each subject rested on the shocker plate for 10 s continuously. (A) Duration run until exhaustion. (B) Distance run until exhaustion. Sample sizes were as follows: n=7 for Sirt1flox mice, n=5 for Sirt1flox Tie2-Cre mice, n=7 for Sirt1flox MCK-PGC1α mice, and n=7 for Sirt1flox MCK-PGC1α Tie2-Cre mice. Asterisks indicate statistical significance at $p<0.05$.

Aim 3 Results

The murine MS1 endothelial cell line, which is more readily propagated than primary endothelial cells and can be used in a variety of *in vitro* angiogenesis assays, was used to investigate possible mechanisms by which Sirt1 regulates angiogenic behavior within endothelial cells.

siRNA decreases expression of Sirt1 in MS1 cells

Transfection of MS1 cells with Sirt1 siRNA was found to effectively decrease Sirt1 expression. RT-qPCR analysis demonstrated that Sirt1 knockdown using siRNA resulted in a 62.4±7.0% decrease in mRNA content for Sirt1 exon 4 (**Figure 19A**) compared to cells treated with scrambled (negative control) siRNA. Furthermore, Western blotting demonstrated that knockdown using siRNA resulted in a mean decrease of 76.0% in Sirt1 protein content (**Figure 19B**) compared to cells treated with scrambled siRNA. Knockdown was also apparent at the protein level by immunofluorescence for Sirt1 (**Figure 19C**).
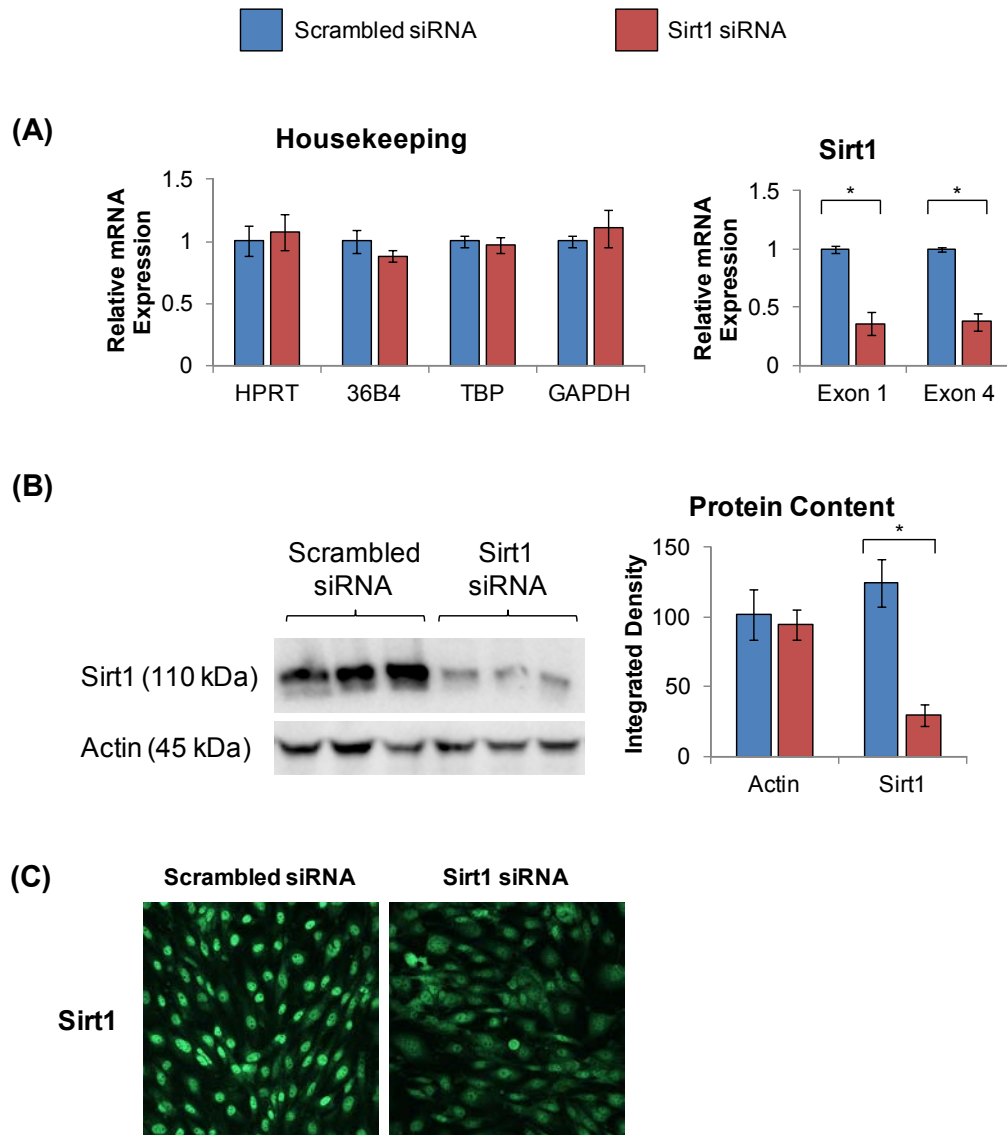
Figure 19: Treatment of MS1 endothelial cells with Sirt1 siRNA decreases expression of Sirt1 at the mRNA and protein levels.

MS1 endothelial cells were transfected with Sirt1 siRNA vs. scrambled siRNA (negative control). (A) Total mRNA was isolated from the MS1 cells at 24 h after transfection, and then analyzed by RT-qPCR (n=4 for each condition). mRNA expression levels of housekeeping genes (left panel) and Sirt1 (right panel) were quantified. (B) MS1 cells were lysed 24 h after transfection for analysis by Western blotting. Western blots showing protein levels of Sirt1 (left panel) and quantification of integrated band density (n=3 for each condition). GAPDH was used as a loading control. (C) Representative images of Sirt1 immunofluorescence after MS1 cells were fixed at 24 h after transfection. Asterisks indicate statistical significance at $p<0.05$.

Migration of MS1 endothelial cells is impaired by knockdown of Sirt1

MS1 cells treated with Sirt1 siRNA exhibited significantly decreased migration into the "wound" area in an *in vitro* scratch assay (**Figure 20**) compared to MS1 cells treated with scrambled siRNA (negative control).

(A)

(B)
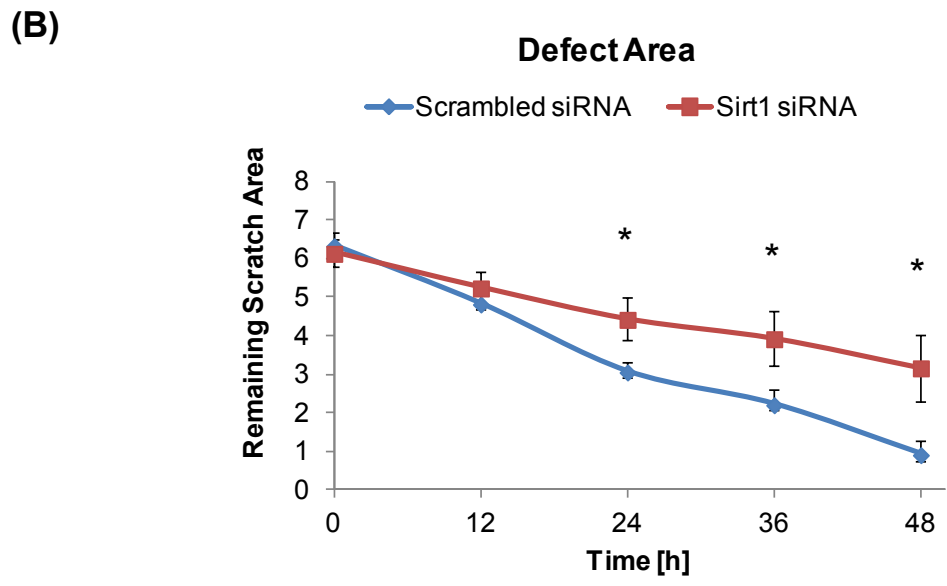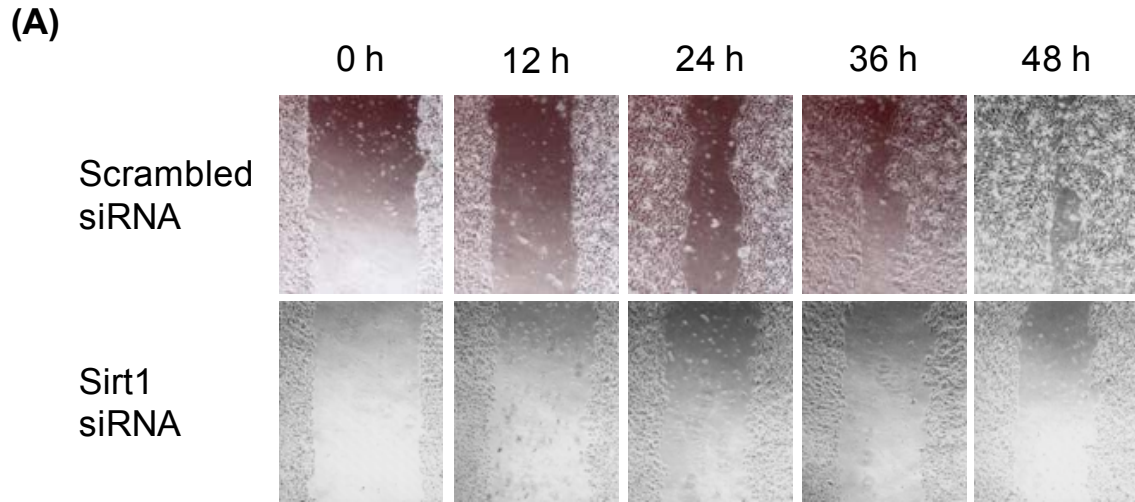
Figure 20: Sirt1 knockdown decreases migration of MS1 cells in an *in vitro* scratch assay.

MS1 endothelial cells were transfected with Sirt1 siRNA vs. scrambled siRNA (negative control) and then subjected to an *in vitro* "wound healing" assay. (A) Representative brightfield microscopy images showing migration of cells into the scratch area over 48 h. (B) Quantification of scratch assay results (n=4 for each treatment). Asterisks indicate statistical significance at $p < 0.05$.

Furthermore, in a Transwell cell migration assay, MS1 cells treated with Sirt1 siRNA exhibited decreased chemotaxis in response to VEGF and to conditioned media produced by C2C12 myotubes transduced with an adenoviral overexpression vector for PGC1α (**Figure 21**), compared to MS1 cells treated with scrambled siRNA (negative control).

Thus, *in vitro* angiogenesis assays demonstrated that Sirt1 knockdown in MS1 endothelial cells resulted in impaired cell migration in response to angiogenic factors, similar to the *in vivo* findings in mice with endothelial-specific knockout of Sirt1 catalytic activity.

Transswell Migration Assay
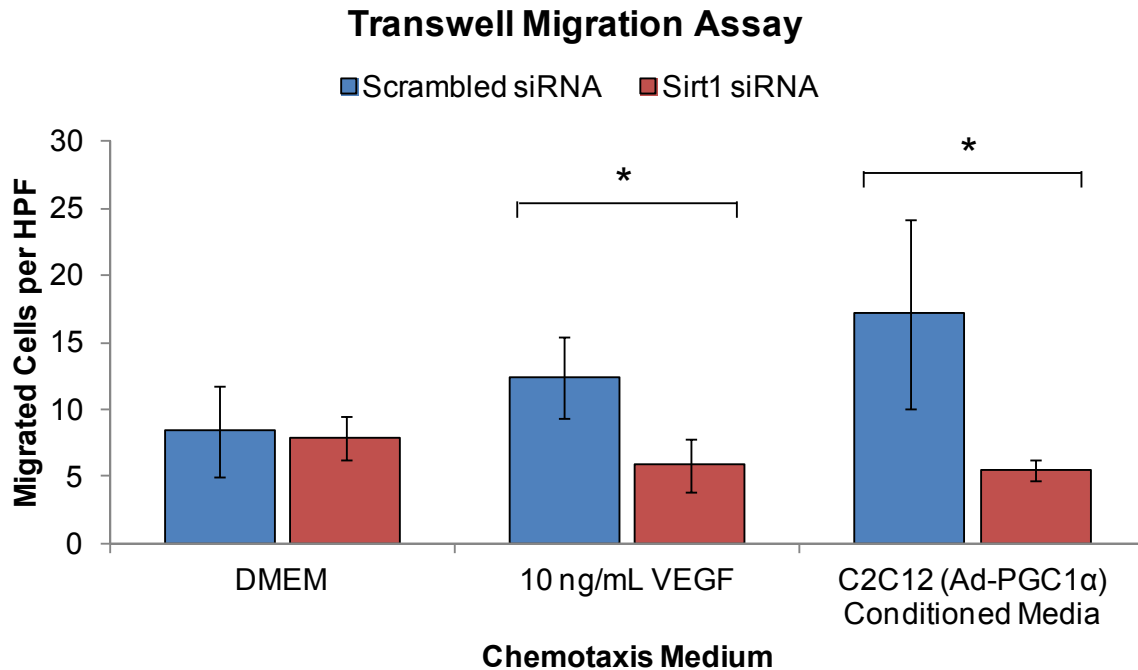
Figure 21: Sirt1 knockdown decreases chemotaxis of MS1 cells in Transwell migration assay.

MS1 endothelial cells were transfected with Sirt1 siRNA vs. scrambled siRNA (negative control) and then subjected to a Transwell migration assay using 10 ng/mL VEGF or conditioned media from C2C12s transduced with Adeno-PGC1α as a chemoattractant. The number of migrated cells per high power field was quantified (n=4 for each condition). Asterisks indicate statistical significance at $p<0.05$.

Chemotaxis of MS1 endothelial cells is still impaired by knockdown of Sirt1 in the absence of Notch signaling

MS1 cells were then treated with DAPT (a gamma-secretase inhibitor that abrogates Notch signaling) as well as transfected with Sirt1 siRNA in order to evaluate whether Sirt1 regulates angiogenic behavior of MS1 cells through modulating Notch signaling.

Sirt1 knockdown by siRNA and inhibition of Notch signaling by DAPT treatment were confirmed by RT-qPCR (**Figure 22A**). In a Transwell cell migration assay, MS1 cells transfected with Sirt1 siRNA again exhibited decreased chemotaxis in response to VEGF compared to MS1 cells transfected with scrambled siRNA, as expected. Interestingly,

transfecting MS1 cells with Sirt1 siRNA led to decreased cell migration compared to transfecting cells with scrambled siRNA, even when Notch signaling was inhibited by DAPT (**Figure 22B**). Thus, in MS1 endothelial cells, Sirt1 appears to regulate chemotaxis through Notch-independent pathways, which remain to be characterized.
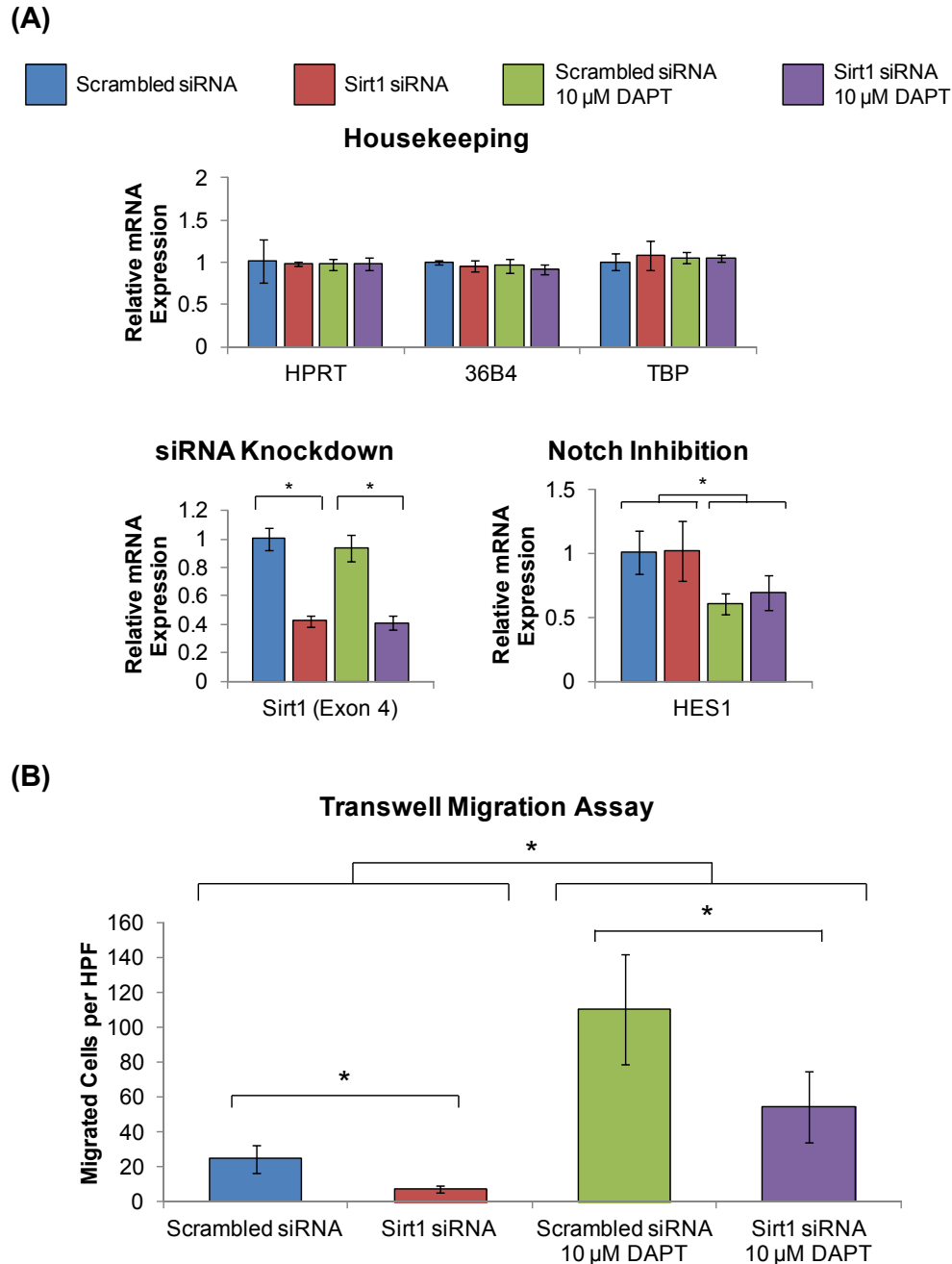
Figure 22: Sirt1 knockdown decreases chemotaxis of MS1 cells even in when Notch signaling has been inhibited.

MS1 endothelial cells were simultaneously transfected with Sirt1 siRNA vs. scrambled siRNA and treated with the γ-secretase inhibitor DAPT. (A) mRNA expression levels of housekeeping genes (left panel), Sirt1 (middle panel), and the Notch target HES1 (right panel) (n=4 for each condition). (B) MS1 cells were then subjected to a Transwell migration assay using 10 ng/mL VEGF as a chemoattractant, and the number of migrated cells was quantified (n=6 for each condition). Asterisks indicate statistical significance at $p < 0.05$.

DISCUSSION

Sirt1 within skeletal myofibers is not required for the activity of PGC1α when PGC1α is overexpressed *in vivo*.

In this study, we demonstrate that Sirt1 within skeletal myofibers is not required for the activity of PGC1α when PGC1α is overexpressed in skeletal myofibers *in vivo*. A major limitation of this discovery is that we did not perform mass spectrometry to compare, between Sirt1flox MCK-PGC1α Myog-Cre and Sirt1flox MCK-PGC1α mice, the acetylation status of each of 13 lysine residues at which PGC1α has been reported to be acetylated,(7) therefore it remains to be seen whether deacetylation in itself is not required for PGC1α activity in skeletal myofibers or whether other proteins with deacetylase activity are compensating for knockout of Sirt1 in skeletal myofibers. Furthermore, although we demonstrated deletion of Sirt1 exon 4 in whole tissue samples (at the gDNA, mRNA, protein levels), we did not perform experiments using isolated teased skeletal myofibers, therefore we cannot calculate the efficiency of knockout of Sirt1 exon 4 in myofibers alone.

Our methods address several pitfalls faced by groups who have previously sought to investigate the regulation of PGC1α by Sirt1 in skeletal muscle. First, in contrast to several other groups,(14-16) our experiments are performed either entirely *in vivo* using tissues freshly harvested from sacrificed mice or *in vitro* using differentiated primary myotubes, rather than *in vitro* using the immortalized C2C12 myoblast cell line. Indeed, that our findings differ from studies using C2C12 cells suggests that this cell line may not accurately reflect all aspects of *in vivo* molecular physiology. Second, in contrast to Philp et al.,(24) we confirm deletion of Sirt1 exon 4 at the protein level by Western blotting, and specifically demonstrate the presence of the shortened Sirt1 variant (ΔExon 4) in whole quadriceps lysates from Sirt1flox Myog-Cre mice. Third, in contrast to Menzies et al.,(22) we transgenically overexpressed PGC1α in skeletal myofibers in order to simulate exercise training. The Sirt1flox MCK-PGC1α mice serve as a clear positive control in our experiments, thereby overcoming ambiguities raised by the recent discovery that exercise-induced mitochondrial biogenesis is preserved in mice lacking PGC1α in skeletal myofibers.(23) Furthermore, overexpression of PGC1α within skeletal myofibers provides a direct *in vivo* counterpart to previous *in vitro* studies wherein PGC1α was overexpressed in C2C12 myotubes using adenoviral vectors.(14, 15) Here, however, it is

important to concede that it is possible that transgenic overexpression of PGC1α could overwhelm the acetylation machinery of skeletal myofibers *in vivo*, therefore it remains to be seen if Sirt1 within skeletal myofibers has a role in regulating PGC1α under true physiologic conditions, for example when PGC1α is acutely induced in skeletal myofibers in response to exercise training.

Interestingly, we did not detect decreases in expression of mitochondrial-encoded genes of oxidative phosphorylation upon deletion of Sirt1 exon 4 in skeletal myofibers, which stands in contrast to results reported by some previous groups. Specifically, Gomes et al. found decreased expression of mitochondrial-encoded genes in skeletal muscle samples from whole body Sirt1 exon 4 mice (Sirt1flox ERT2-Cre).(21) The reduction in expression of mitochondrial-encoded genes appears to become more pronounced with age, as Chalkiadaki et al. detected only a slight reduction in gene expression of approximately 10% in 3-to-4-month old mice with skeletal myofiber-specific deletion of Sirt1 exon 4 (Sirt1flox MCK-Cre), leading them to ultimately conclude that "Sirt1 is dispensable for the expression of mitochondrial genes,"(25) while Gomes et al. detected a more substantial reduction of approximately 60% in 6-to-10-month old mice.(21) In our studies, we most likely did not detect a reduction in mitochondrial-encoded genes because we harvested whole muscle samples from mice at the age of 4 months, when decreases in mRNA expression of mitochondrial genes between Sirt1flox and Sirt1flox Myog-Cre cohorts were slight (similar to Chalkiadaki et al.). Of note, we did detect decreases in mRNA expression of some mitochondrial-encoded genes in whole quadriceps samples from Sirt1flox Myog-Cre mice compared to Sirt1flox mice (27.5% reduction in ND5 and 42.9% reduction in CytB, see **Figure 8B**), but these decreases were not statistically significant.

Furthermore, Chalkiadaki et al. observed that Sirt1flox MCK-Cre mice exhibited significantly decreased endurance capacity compared to Sirt1flox mice upon treadmill testing.(25) Interestingly, they found these differences exclusively under a high stress endurance testing protocol. However, the treadmill endurance testing protocol used in our studies (which we have optimized to yield consistent and reproducible results) is nearly identical to the low stress protocol used by Chalkiadaki et al, for which they observed no differences between Sirt1flox MCK-Cre mice and Sirt1flox mice.(25)

Sirt1 within endothelial cells is required for angiogenesis in response to PGC1α overexpression *in vivo*.

In this study, we also definitively demonstrate that endothelial Sirt1 is required for angiogenesis in response to PGC1α, an essential mediator of exercise-induced angiogenesis in skeletal muscle. In addition, we report that deletion of endothelial Sirt1 activity does not affect the ability of PGC1α overexpressed in skeletal myofibers to upregulate mRNA expression of genes of oxidative metabolism or proteins of oxidative phosphorylation in skeletal muscle tissue – a finding that is not altogether surprising given that, in this context, PGC1α is coactivating gene expression in the skeletal myofibers within which it is produced, without need for additional factors produced by endothelial cells.

Interestingly, Sirt1flox MCK-PGC1α Tie2-Cre mice simultaneously exhibit decreased capillary density in quadriceps cross-sections as well as decreased treadmill exercise performance compared to Sirt1flox MCK-PGC1α mice, thus the results of our quantification of vascular density parallel those of our treadmill endurance testing. We cannot conclude whether the decreased exercise performance in Sirt1flox MCK-PGC1α Tie2-Cre was solely caused by decreased density of the skeletal muscle vasculature, as opposed to intrinsic dysfunction of the endothelium (e.g. impaired nutrient transport) caused by loss of Sirt1 catalytic activity. However, we speculate that intrinsic endothelial dysfunction does not make the chief contribution to this phenotype, because no significant differences in treadmill endurance were observed between Sirt1flox Tie2-Cre mice and Sirt1flox mice, groups which did not overexpress PGC1α.

Moreover, our finding that Sirt1 is required for PGC1α-induced angiogenesis contributes to a larger of body of work identifying endothelial Sirt1 as a key regulator of angiogenesis in many tissues throughout the body. Much work has been done in the past decade to characterize small molecules that act as Sirt1 activating compounds (STACs)(30, 31) and the endothelium is readily bioavailable when drugs are delivered by intravenous or intra-arterial injection, therefore our work highlights endothelial Sirt1 as an exciting new target for treating vascular diseases. We are optimistic that pharmacologically modulating endothelial Sirt1 activity has therapeutic potential for peripheral artery disease, myocardial ischemia, and even vascular diseases of the central nervous system (e.g. vascular depression and vascular dementia).

Sirt1 regulates chemotaxis in MS1 endothelial cells by signaling through Notch-independent pathways

The murine MS1 endothelial cell line is a convenient tool for conducting preliminary *in vitro* experiments to probe the mechanisms by which Sirt1 regulates angiogenic behavior of endothelial cells. A caveat of this method is that the MS1 line is, of course, an immortalized cell line and therefore may not accurately reflect the physiology of endothelial cells *in vivo*. Importantly, we found that MS1 cells do appear to recapitulate *in vivo* physiology in that they exhibit impaired chemotaxis when Sirt1 expression is knocked down using siRNA. Furthermore, we report here that, in MS1 endothelial cells, Sirt1 appears to regulate chemotaxis through targeting Notch-independent pathways. A diagram which summarizes our proposed model for the role of endothelial Sirt1 in skeletal muscle tissue is shown in **Figure 23**.
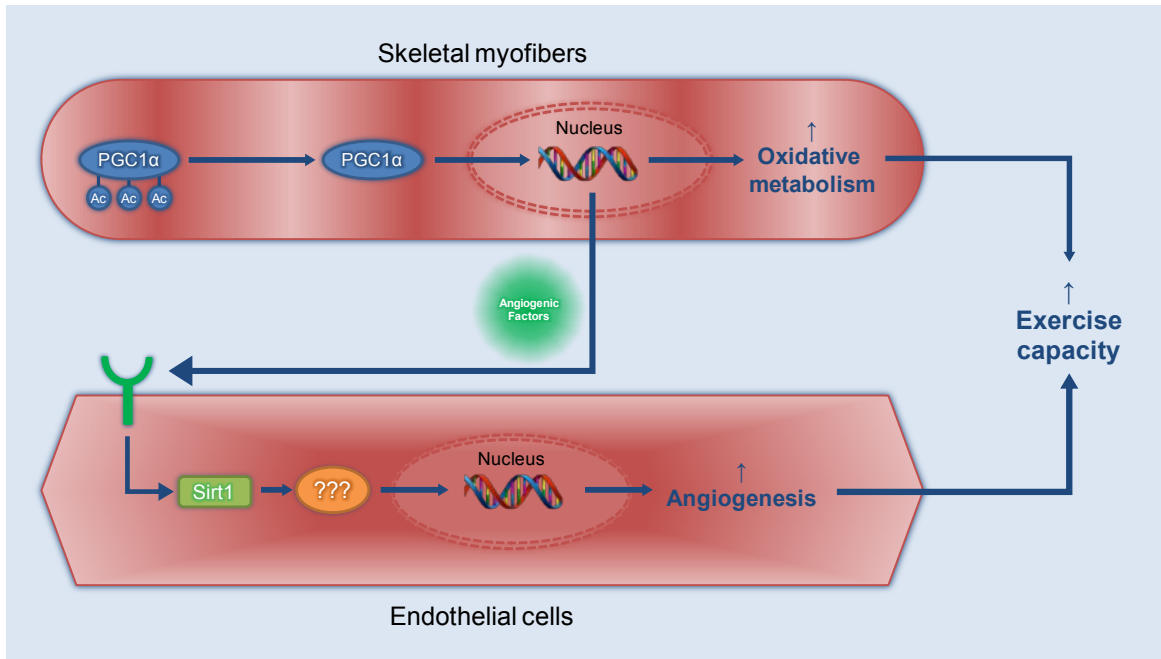
Figure 23: A new proposed model of role of Sirt1 in regulating adaptations of skeletal muscle tissue to PGC1α *in vivo*.

Sirt1 within skeletal myofibers is not required for upregulation of mitochondrial biogenesis and secretion of angiogenic factors in response to PGC1α. In contrast, Sirt1 within endothelial cells is required for angiogenesis in response to angiogenic factors secreted in response to PGC1α. Endothelial Sirt1 may regulate angiogenic behavior by modulating targets independent of the Notch pathway, which remain to be characterized.

The role of Notch signaling in angiogenesis is highly complex. Specifically, inhibition of Notch1 signaling is critical for formation of endothelial tip cells (specialized endothelial cells that extend filopodia and lead outgrowth of blood vessels toward gradients of angiogenic factors), yet active Notch1 signaling is required for the differentiation of endothelial stalk cells (specialized endothelial cells that follow tip cells, establish tight junctions, and proliferate to form the nascent vascular lumen).(32) Thus, in order to maintain appropriate patterns of sprouting and branching during angiogenesis, Notch signaling must be coordinately inhibited in tip cells but permitted in stalk cells.(32) Consequently, Notch inhibitors such as DAPT are not viable candidates for treating diseases of vascular insufficiency because, although inhibition of Notch signaling enhances angiogenesis, the resulting capillary beds exhibit non-physiologic

branching patterns, markedly reduced size of the vessel lumen, and ultimately worse perfusion.(33, 34)

Our finding that Sirt1 modulates chemotaxis via Notch-independent pathways in MS1 endothelial cells thus builds our enthusiasm that endothelial Sirt1 is potential therapeutic target for diseases of vascular insufficiency. In fact, although it is beyond the scope of this thesis, our preliminary observations of mice that overexpress Sirt1 specifically in endothelial cells (Sirt1tg Tie2-Cre) suggest that capillary density of skeletal muscle is increased in a physiologic manner that promotes tissue perfusion. Nonetheless, our studies using MS1 endothelial cells are highly preliminary and much further work, using both *in vitro* and *in vivo* models, is necessary to clarify the exact molecular pathways by which endothelial Sirt1 modulates angiogenesis. In this regard, it will be very interesting to learn how Sirt1 and Notch signaling converge to influence angiogenic behavior within endothelial cells.

Future Directions

Our future studies will seek to evaluate the potential of endothelial Sirt1 as a therapeutic target for diseases of vascular insufficiency. While several STACs have been identified which directly increase the affinity of Sirt1 for its peptide substrates,(30, 31) their therapeutic potential is unclear that the bioavailability of NAD^+, the co-substrate for the deacetylation reaction catalyzed by Sirt1, declines significantly in human tissues during aging.(21, 35, 36) Alternatively, a promising strategy for treating vascular disease through augmenting the activity of Sirt1 is to pharmacologically increase the availability of NAD^+. One molecule we are investigating is nicotinamide mononucleotide (NMN), an endogenous precursor of NAD^+ which is converted intracellularly into NAD^+ by nicotinamide mononucleotide adenylyltransferase (NMNAT) (see **Figure 24**). Previous studies have demonstrated that intraperitoneal injection of NMN in mice is capable of raising NAD^+ levels in the liver, adipose tissue, and skeletal muscle tissue.(21, 37) Furthermore, a recent study using human aortic endothelial cells reported that transgenic overexpression of nicotinamide phosphoribosyltransferase (NAMPT, the enzyme which converts nicotinamide into NMN) enhances tube formation, suggesting that increasing NAD^+ levels within endothelial cells can improve their angiogenic capacity *in vitro*.(38) Thus, we propose that pharmacologically raising NAD^+ levels by supplementing endothelial cells with exogenous NMN may enhance angiogenesis *in vivo*.

Currently, we are characterizing the effects of administering NMN in mouse models of hindlimb ischemia caused by femoral artery ligation and in mice with age-associated endothelial dysfunction. Importantly, any positive results we find in wildtype mice will be repeated in mice lacking endothelial Sirt1 activity (Sirt1flox Tie2-Cre) to confirm that the effects of NMN are indeed mediated by Sirt1 within endothelial cells. If these studies ultimately demonstrate that pharmacologic activators of Sirt1 are capable of enhancing angiogenesis *in vivo*, further studies will be required to develop strategies to deliver these drugs to the endothelium within target organs and well as to better characterize adverse effects of these drugs (for example, enhanced growth of solid tumors is a potential adverse effect of concern that will need to be studied comprehensively).
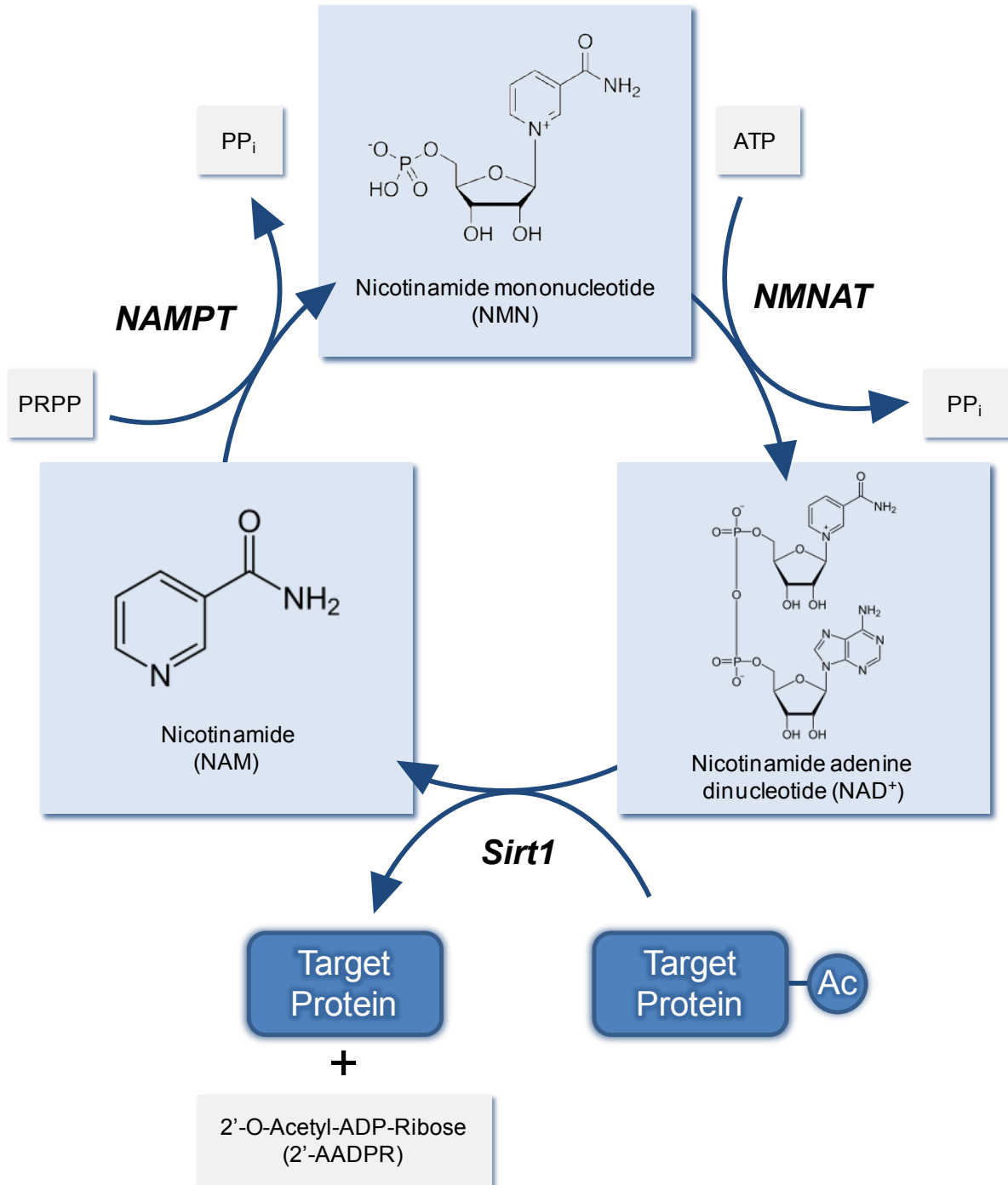
Figure 24: The NAD$^+$ Salvage Pathway

Nicotinamide mononucleotide (NMN) is converted into nicotinamide adenine dinucleotide (NAD$^+$) by the nicotinamide adenine dinucleotide adenylyltransferase (NMNAT). NAD$^+$ then serves as a substrate for the Sirt1-mediated deacetylation reaction, resulting in the production of 2'-O-acetyl-ADP-ribose (2'-AADPR) and nicotinamide (NAM).

CONCLUSIONS

In this study, we report the following novel findings:

1. Sirt1 within skeletal myofibers is not required for the activity of PGC1α when PGC1α is overexpressed *in vivo*.

2. Sirt1 within endothelial cells is required for angiogenesis in skeletal muscle tissue in response to PGC1α overexpression *in vivo*.

3. In MS1 endothelial cells, Sirt1 regulates chemotaxis through Notch-independent pathways.

Ultimately, these discoveries identify endothelial Sirt1 as a key regulator of angiogenesis in skeletal muscle tissue and as a potential therapeutic target for diseases of vascular insufficiency. Consequently, our future studies will explore the use of pharmacologic activators of Sirt1 to enhance angiogenesis for therapeutic purposes.

LAY SUMMARY

The health benefits of regular exercise include decreased risk of cardiovascular disease, decreased risk of type II diabetes, prevention of age-associated muscle wasting, and resolution of chronic inflammation. It is believed that these health benefits are mediated in part by the adaptations of skeletal muscle tissue to exercise. Precisely how our bodies sense exercise and then coordinate the physiologic adaptations of skeletal muscle tissue to exercise are subjects of intense investigation.

Sirtuin 1 (Sirt1), which is well-known for its role in extending lifespan in lower organisms in response to caloric restriction, is a protein with deacetylase activity that regulates cellular energy output throughout the body. Based on studies using immortalized myoblast cells, it has been widely assumed that Sirt1 within skeletal myofibers (the cells which contain contractile elements of skeletal muscle) is required for activating PGC1α, a metabolic regulator that is potently induced by exercise and functions to increase aerobic metabolism and direct the formation of new capillaries in muscle tissue. However, this role of Sirt1 within skeletal myofibers has not yet been confirmed in living animals. Recent work also suggests that Sirt1 within endothelial cells (the cells which line the interior of blood vessels) may promote new blood vessel formation throughout the body by inhibiting signaling through the Notch pathway. However, the role of endothelial Sirt1 in regulating angiogenesis (the formation of new capillaries from preexisting blood vessels) in skeletal muscle has not yet been investigated. We propose that Sirt1 in skeletal myofibers is not required for activity of PGC1α, and we hypothesize instead that Sirt1 within endothelial cells is required for angiogenesis within skeletal muscle tissue in response to PGC1α.

To investigate this hypothesis, we generated mice that lack Sirt1 activity in either skeletal myofibers or in endothelial cells, and overexpressed PGC1α in skeletal muscle in order to simulate exercise training. By measuring the abilities of PGC1α to upregulate oxidative metabolism at the mRNA and protein levels, to promote formation of new capillaries in skeletal muscle, and to increase treadmill endurance performance, we show that the activity PGC1α is not compromised by loss of Sirt1 activity in skeletal myofibers. In contrast, we observe that loss of Sirt1 activity in endothelial cells results in decreased formation of new capillaries in response to PGC1α. Thus, we conclude that Sirt1 within skeletal myofibers is not required for the activity

of PGC1α in mouse models where PGC1α is overexpressed; however, endothelial Sirt1 is required for angiogenesis in skeletal muscle tissue in response to PGC1α overexpression. Furthermore, our experiments using a mouse endothelial cell line reveal that, within endothelial cells, Sirt1 regulates cell migration by signaling through Notch-independent pathways.

Ultimately, these findings identify Sirt1 within endothelial cells as a new target for treating diseases of vascular insufficiency. Our current studies now seek to determine if using small molecules to pharmacologically activate Sirt1 can enhance outcomes of vascular disease in mouse models. This has therapeutic potential for peripheral artery disease, myocardial ischemia, and vascular diseases of the central nervous system.

ABBREVIATIONS

36B4 = ribosomal protein, large, P0

Adeno = adenoviral-mediated overexpression

ATP5o = ATP synthase subunit O

BSA = bovine serum albumin

C2C12 = mouse myoblast cell line

cDNA = complementary DNA

Cox = cytochrome C oxidase

CPT1B = Carnitine palmitoyltransferase 1B

Cre = Cre recombinase

CS = citrate synthase

CYCS = cytochrome C, somatic

CytB = cytochrome B

Da = dalton

DAPI = 4',6-diamidino-2-phenylindole

DAPT = gamma-secretase inhibitor

DMEM = Dulbecco's modified eagle medium

ERR = estrogen-related receptor

FITC = fluorescein isothiocyanate

flox = flanked by LoxP recombination sequences

FOXO = Forkhead box

GAPDH = glyceraldehydes-3-phosphate dehydrogenase

gDNA = genomic DNA

GFP = green fluorescent protein

HPRT = hypoxanthine-guanine phosphoribosyltransferase

HRP = horseradish peroxidase

HUVEC = human umbilical vein endothelial cell

IACUC = institutional animal care and use committee

IDV = integrated density value

LXR = liver X receptor

Lys = lysine

MCAD = medium-chain acyl-coenzyme A dehydrogenase

MCK = muscle creatine kinase

MEM = minimal essential medium

MOI = multiplicity of infection

mRNA = messenger RNA

MS1 = mouse endothelial cell line

Myog = myogenin

Myog-Cre = Cre recombinase gene under expression of Myog promoter

NAD = nicotinamide adenine dinucleotide

ND = mitochondrial-encoded NADH dehydrogenase

NDUFB4 = NADH dehydrogenase 1β subcomplex 5

NICD = Notch intracellular domain

NMN = nicotinamide mononucleotide

NMN = nicotinamide mononucleotide adenylyltransferase

PGC1α = peroxisome proliferator-activated receptor-γ coactivator-1α

MCK-PGC1α = PGC1α gene under expression of MCK promoter

PGC1β = peroxisome proliferator-activated receptor-γ coactivator-1β

PBS = phosphate-buffered saline

PRC = PGC-related coactivator

qPCR = quantitative polymerase chain reaction

RPM = revolutions per minute

RT-qPCR = quantitative reverse transcription polymerase chain reaction

Sirt = Sirtuin

Sirt1flox = Sirt1 gene with exon 4 flanked by LoxP sequences

siRNA = short interfering RNA

STAC = Sirt1 activating compound

TBP = TATA-box binding protein

TBST = tris-buffered saline with tween

TFAM = transcription factor A, mitochondrial

Tie2 = angiopoietin receptor 2

Tie2-Cre = Cre recombinase gene under expression of Tie2 promoter

VEGF = vascular endothelial growth factor A

WT = wildtype

REFERENCES

1.   Dillon LM, Rebelo AP, Moraes CT. The role of PGC-1 coactivators in aging skeletal muscle and heart. IUBMB life. 2012;64(3):231-41. Epub 2012/01/27. doi: 10.1002/iub.608. PubMed PMID: 22279035; PubMed Central PMCID: PMC4080206.

2.   Handschin C, Spiegelman BM. The role of exercise and PGC1alpha in inflammation and chronic disease. Nature. 2008;454(7203):463-9. Epub 2008/07/25. doi: 10.1038/nature07206. PubMed PMID: 18650917; PubMed Central PMCID: PMC2587487.

3.   Wenz T, Rossi SG, Rotundo RL, Spiegelman BM, Moraes CT. Increased muscle PGC-1alpha expression protects from sarcopenia and metabolic disease during aging. Proceedings of the National Academy of Sciences of the United States of America. 2009;106(48):20405-10. Epub 2009/11/18. doi: 10.1073/pnas.0911570106. PubMed PMID: 19918075; PubMed Central PMCID: PMC2787152.

4.   Haigis MC, Sinclair DA. Mammalian sirtuins: biological insights and disease relevance. Annual review of pathology. 2010;5:253-95. Epub 2010/01/19. doi: 10.1146/annurev.pathol.4.110807.092250. PubMed PMID: 20078221; PubMed Central PMCID: PMC2866163.

5.   Lin SJ, Defossez PA, Guarente L. Requirement of NAD and SIR2 for life-span extension by calorie restriction in Saccharomyces cerevisiae. Science. 2000;289(5487):2126-8. Epub 2000/09/23. PubMed PMID: 11000115.

6.   Rogina B, Helfand SL. Sir2 mediates longevity in the fly through a pathway related to calorie restriction. Proceedings of the National Academy of Sciences of the United States of America. 2004;101(45):15998-6003. Epub 2004/11/03. doi: 10.1073/pnas.0404184101. PubMed PMID: 15520384; PubMed Central PMCID: PMC528752.

7.   Rodgers JT, Lerin C, Haas W, Gygi SP, Spiegelman BM, Puigserver P. Nutrient control of glucose homeostasis through a complex of PGC-1alpha and SIRT1. Nature. 2005;434(7029):113-8. Epub 2005/03/04. doi: 10.1038/nature03354. PubMed PMID: 15744310.

8.   Nemoto S, Fergusson MM, Finkel T. SIRT1 functionally interacts with the metabolic regulator and transcriptional coactivator PGC-1{alpha}. The Journal of biological chemistry. 2005;280(16):16456-60. Epub 2005/02/18. doi: 10.1074/jbc.M501485200. PubMed PMID: 15716268.

9.   Anderson RM, Barger JL, Edwards MG, Braun KH, O'Connor CE, Prolla TA, et al. Dynamic regulation of PGC-1alpha localization and turnover implicates mitochondrial adaptation in calorie restriction and the stress response. Aging cell. 2008;7(1):101-11. Epub 2007/11/23. doi: 10.1111/j.1474-9726.2007.00357.x. PubMed PMID: 18031569; PubMed Central PMCID: PMC2253697.

10.   Pilegaard H, Saltin B, Neufer PD. Exercise induces transient transcriptional activation of the PGC-1alpha gene in human skeletal muscle. The Journal of physiology. 2003;546(Pt 3):851-8. Epub 2003/02/04. PubMed PMID: 12563009; PubMed Central PMCID: PMC2342594.

11.   Miura S, Kawanaka K, Kai Y, Tamura M, Goto M, Shiuchi T, et al. An increase in murine skeletal muscle peroxisome proliferator-activated receptor-gamma coactivator-1alpha (PGC-1alpha) mRNA in response to exercise is mediated by beta-adrenergic receptor activation. Endocrinology. 2007;148(7):3441-8. Epub 2007/04/21. doi: 10.1210/en.2006-1646. PubMed PMID: 17446185.

12.   Calvo JA, Daniels TG, Wang X, Paul A, Lin J, Spiegelman BM, et al. Muscle-specific expression of PPARgamma coactivator-1alpha improves exercise performance and increases peak oxygen uptake. J Appl Physiol (1985). 2008;104(5):1304-12. Epub 2008/02/02. doi: 10.1152/japplphysiol.01231.2007. PubMed PMID: 18239076.

13.   Chinsomboon J, Ruas J, Gupta RK, Thom R, Shoag J, Rowe GC, et al. The transcriptional coactivator PGC-1alpha mediates exercise-induced angiogenesis in skeletal muscle. Proceedings of the National Academy of Sciences of the United States of America. 2009;106(50):21401-6. Epub 2009/12/08. doi: 10.1073/pnas.0909131106. PubMed PMID: 19966219; PubMed Central PMCID: PMC2795492.

14.   Lagouge M, Argmann C, Gerhart-Hines Z, Meziane H, Lerin C, Daussin F, et al. Resveratrol improves mitochondrial function and protects against metabolic disease by activating SIRT1 and PGC-1alpha. Cell. 2006;127(6):1109-22. Epub 2006/11/23. doi: 10.1016/j.cell.2006.11.013. PubMed PMID: 17112576.

15.   Gerhart-Hines Z, Rodgers JT, Bare O, Lerin C, Kim SH, Mostoslavsky R, et al. Metabolic control of muscle mitochondrial function and fatty acid oxidation through SIRT1/PGC-1alpha. The EMBO journal. 2007;26(7):1913-23. Epub 2007/03/10. doi: 10.1038/sj.emboj.7601633. PubMed PMID: 17347648; PubMed Central PMCID: PMC1847661.

16.   Canto C, Gerhart-Hines Z, Feige JN, Lagouge M, Noriega L, Milne JC, et al. AMPK regulates energy expenditure by modulating NAD+ metabolism and SIRT1 activity. Nature. 2009;458(7241):1056-60. Epub 2009/03/06. doi: 10.1038/nature07813. PubMed PMID: 19262508; PubMed Central PMCID: PMC3616311.

17.   Gurd BJ, Little JP, Perry CG. Does SIRT1 determine exercise-induced skeletal muscle mitochondrial biogenesis: differences between in vitro and in vivo experiments? J Appl Physiol (1985). 2012;112(5):926-8. Epub 2011/11/19. doi: 10.1152/japplphysiol.01262.2011. PubMed PMID: 22096123.

18.   Menzies KJ, Chabi B, Hood DA, Schenk S, Philp A, Braga VA, et al. Commentaries on viewpoint: does SIRT1 determine exercise-induced skeletal muscle mitochondrial biogenesis: differences between in vitro and in vivo experiments? J Appl Physiol (1985). 2012;112(5):929-30. Epub 2012/03/03. doi: 10.1152/japplphysiol.00094.2012. PubMed PMID: 22383496.

19.   Gurd BJ, Little JP, Perry CG. Last word on viewpoint: does SIRT1 determine exercise-induced skeletal muscle mitochondrial biogenesis: differences between in vitro and in vivo experiments? J Appl Physiol (1985). 2012;112(5):931. Epub 2012/03/03. doi: 10.1152/japplphysiol.00078.2012. PubMed PMID: 22383497.

20.   Cheng HL, Mostoslavsky R, Saito S, Manis JP, Gu Y, Patel P, et al. Developmental defects and p53 hyperacetylation in Sir2 homolog (SIRT1)-deficient mice. Proceedings of the National Academy of Sciences of the United States of America. 2003;100(19):10794-9. Epub 2003/09/10. doi: 10.1073/pnas.1934713100. PubMed PMID: 12960381; PubMed Central PMCID: PMC196882.

21.   Gomes AP, Price NL, Ling AJ, Moslehi JJ, Montgomery MK, Rajman L, et al. Declining NAD(+) induces a pseudohypoxic state disrupting nuclear-mitochondrial communication during aging. Cell. 2013;155(7):1624-38. Epub 2013/12/24. doi: 10.1016/j.cell.2013.11.037. PubMed PMID: 24360282; PubMed Central PMCID: PMC4076149.

22.   Menzies KJ, Singh K, Saleem A, Hood DA. Sirtuin 1-mediated effects of exercise and resveratrol on mitochondrial biogenesis. The Journal of biological chemistry. 2013;288(10):6968-79. Epub 2013/01/19. doi: 10.1074/jbc.M112.431155. PubMed PMID: 23329826; PubMed Central PMCID: PMC3591607.

23.   Rowe GC, El-Khoury R, Patten IS, Rustin P, Arany Z. PGC-1alpha is dispensable for exercise-induced mitochondrial biogenesis in skeletal muscle. PloS one. 2012;7(7):e41817. Epub 2012/08/01. doi: 10.1371/journal.pone.0041817. PubMed PMID: 22848618; PubMed Central PMCID: PMC3404101.

24.   Philp A, Chen A, Lan D, Meyer GA, Murphy AN, Knapp AE, et al. Sirtuin 1 (SIRT1) deacetylase activity is not required for mitochondrial biogenesis or peroxisome proliferator-activated receptor-gamma coactivator-1alpha (PGC-1alpha) deacetylation following endurance exercise. The Journal of biological chemistry. 2011;286(35):30561-

70. Epub 2011/07/16. doi: 10.1074/jbc.M111.261685. PubMed PMID: 21757760; PubMed Central PMCID: PMC3162416.

25.   Chalkiadaki A, Igarashi M, Nasamu AS, Knezevic J, Guarente L. Muscle-specific SIRT1 gain-of-function increases slow-twitch fibers and ameliorates pathophysiology in a mouse model of duchenne muscular dystrophy. PLoS genetics. 2014;10(7):e1004490. Epub 2014/07/18. doi: 10.1371/journal.pgen.1004490. PubMed PMID: 25032964; PubMed Central PMCID: PMC4102452.

26.   Potente M, Ghaeni L, Baldessari D, Mostoslavsky R, Rossig L, Dequiedt F, et al. SIRT1 controls endothelial angiogenic functions during vascular growth. Genes & development. 2007;21(20):2644-58. Epub 2007/10/17. doi: 10.1101/gad.435107. PubMed PMID: 17938244; PubMed Central PMCID: PMC2000327.

27.   Guarani V, Deflorian G, Franco CA, Kruger M, Phng LK, Bentley K, et al. Acetylation-dependent regulation of endothelial Notch signalling by the SIRT1 deacetylase. Nature. 2011;473(7346):234-8. Epub 2011/04/19. doi: 10.1038/nature09917. PubMed PMID: 21499261.

28.   Mattagajasingh I, Kim CS, Naqvi A, Yamamori T, Hoffman TA, Jung SB, et al. SIRT1 promotes endothelium-dependent vascular relaxation by activating endothelial nitric oxide synthase. Proceedings of the National Academy of Sciences of the United States of America. 2007;104(37):14855-60. Epub 2007/09/06. doi: 10.1073/pnas.0704329104. PubMed PMID: 17785417; PubMed Central PMCID: PMC1976244.

29.   Xie M, Liu M, He CS. SIRT1 regulates endothelial Notch signaling in lung cancer. PloS one. 2012;7(9):e45331. Epub 2012/10/03. doi: 10.1371/journal.pone.0045331. PubMed PMID: 23028940; PubMed Central PMCID: PMC3445453.

30.   Sinclair DA, Guarente L. Small-molecule allosteric activators of sirtuins. Annual review of pharmacology and toxicology. 2014;54:363-80. Epub 2013/10/29. doi: 10.1146/annurev-pharmtox-010611-134657. PubMed PMID: 24160699; PubMed Central PMCID: PMC4018738.

31.   Hubbard BP, Gomes AP, Dai H, Li J, Case AW, Considine T, et al. Evidence for a common mechanism of SIRT1 regulation by allosteric activators. Science. 2013;339(6124):1216-9. Epub 2013/03/09. doi: 10.1126/science.1231097. PubMed PMID: 23471411; PubMed Central PMCID: PMC3799917.

32.   Hellstrom M, Phng LK, Hofmann JJ, Wallgard E, Coultas L, Lindblom P, et al. Dll4 signalling through Notch1 regulates formation of tip cells during angiogenesis. Nature. 2007;445(7129):776-80. Epub 2007/01/30. doi: 10.1038/nature05571. PubMed PMID: 17259973.

33.   Scehnet JS, Jiang W, Kumar SR, Krasnoperov V, Trindade A, Benedito R, et al. Inhibition of Dll4-mediated signaling induces proliferation of immature vessels and results in poor tissue perfusion. Blood. 2007;109(11):4753-60. Epub 2007/02/22. doi: 10.1182/blood-2006-12-063933. PubMed PMID: 17311993; PubMed Central PMCID: PMC1885521.

34.   Noguera-Troise I, Daly C, Papadopoulos NJ, Coetzee S, Boland P, Gale NW, et al. Blockade of Dll4 inhibits tumour growth by promoting non-productive angiogenesis. Nature. 2006;444(7122):1032-7. Epub 2006/12/22. doi: 10.1038/nature05355. PubMed PMID: 17183313.

35.   Camacho-Pereira J, Tarrago MG, Chini CC, Nin V, Escande C, Warner GM, et al. CD38 Dictates Age-Related NAD Decline and Mitochondrial Dysfunction through an SIRT3-Dependent Mechanism. Cell metabolism. 2016;23(6):1127-39. Epub 2016/06/16. doi: 10.1016/j.cmet.2016.05.006. PubMed PMID: 27304511; PubMed Central PMCID: PMC4911708.

36.   Zhu XH, Lu M, Lee BY, Ugurbil K, Chen W. In vivo NAD assay reveals the intracellular NAD contents and redox state in healthy human brain and their age dependences. Proceedings of the National Academy of Sciences of the United States of America. 2015;112(9):2876-81. Epub 2015/03/03. doi: 10.1073/pnas.1417921112. PubMed PMID: 25730862; PubMed Central PMCID: PMC4352772.

37.   Yoshino J, Mills KF, Yoon MJ, Imai S. Nicotinamide mononucleotide, a key NAD(+) intermediate, treats the pathophysiology of diet- and age-induced diabetes in mice. Cell metabolism. 2011;14(4):528-36. Epub 2011/10/11. doi: 10.1016/j.cmet.2011.08.014. PubMed PMID: 21982712; PubMed Central PMCID: PMC3204926.

38.   Borradaile NM, Pickering JG. Nicotinamide phosphoribosyltransferase imparts human endothelial cells with extended replicative lifespan and enhanced angiogenic capacity in a high glucose environment. Aging cell. 2009;8(2):100-12. Epub 2009/03/24. doi: 10.1111/j.1474-9726.2009.00453.x. PubMed PMID: 19302375.